
Physical Aspects of Computing the Flow of a Viscous Fluid

Unmeel B. Mehta

April 1984

Physical Aspects of Computing the Flow of a Viscous Fluid

Unmeel B. Mehta, Ames Research Center, Moffett Field, California



National Aeronautics and
Space Administration

Ames Research Center
Moffett Field, California 94035

Page intentionally left blank

TABLE of CONTENTS

| | |
|--|----|
| SUMMARY | 1 |
| INTRODUCTION | 1 |
| Brief Historical Background | 1 |
| Future Emphasis | 3 |
| Scope | 5 |
| FLOW REGIMES | 6 |
| Conditions of Incompressibility | 6 |
| Transitional Flows | 7 |
| Turbulent Flows | 9 |
| Navier-Stokes Regime | 10 |
| Non-Navier-Stokes Regime | 11 |
| Thin-shear-layer theory | 11 |
| Viscous-inviscid interaction theory | 13 |
| Composite theory | 15 |
| Shock Waves | 15 |
| Strain Fields | 16 |
| SPATIAL AND TEMPORAL SCALES | 16 |
| Flow Structures in Transitional Flows* | 18 |
| Scales in Turbulent Flows | 20 |
| Organized Structures in Wall-Bounded Turbulent Flows* | 21 |
| Structure of Mean Turbulent Boundary Layer* | 24 |
| Thin- and Slender-Shear Layers | 27 |
| Triple-Deck Region | 27 |
| Shock-Wave/Turbulent-Boundary-Layer Interaction Region | 28 |
| and Trailing Edge of Flat Plate in a Turbulent Flow | |
| Classification of Viscous-Inviscid Interactions | 29 |
| Thickness of Shock Waves | 31 |
| Scales of Strain Rates | 31 |
| Temporal Scales* | 31 |

*Note: Asterisks designate subsections parts of which were published in reference 1.

| | |
|--|----|
| SIGNIFICANCE AND GENERATION OF VORTICITY | 33 |
| Significance of Vorticity | 33 |
| Generation of Vorticity | 34 |
| REFERENCES | 37 |

PHYSICAL ASPECTS OF COMPUTING THE FLOW OF A VISCOUS FLUID

UNMEEL B. MEHTA

SUMMARY

One of the main themes in fluid dynamics at present and in the future is going to be computational fluid dynamics with the primary focus on the determination of drag, flow separation, vortex flows, and unsteady flows. A computation of the flow of a viscous fluid requires an understanding and consideration of the physical aspects of the flow. This is done by identifying the flow regimes and the scales of fluid motion, and the sources of vorticity. Discussions of flow regimes deal with conditions of incompressibility, transitional and turbulent flows, Navier-Stokes and non-Navier-Stokes regimes, shock waves, and strain fields. Discussions of the scales of fluid motion consider transitional and turbulent flows, thin- and slender-shear layers, triple- and four-deck regions, viscous-inviscid interactions, shock waves, strain rates, and temporal scales. In addition, the significance and generation of vorticity are discussed. These physical aspects mainly guide computations of the flow of a viscous fluid.

INTRODUCTION

We have just entered a period when one of the dominant themes in fluid dynamics is going to be computational fluid dynamics. The primary emphasis will be on determining the effects of viscosity, as they relate to drag, flow separation and vortical flows, and unsteady flows. The purpose of this article is to discuss important physical aspects of computing viscous flows.

Brief Historical Background

In the eighteenth century, the Euler equations (ref. 2) governing incompressible inviscid fluid flows were developed. As a consequence of the assumption of inviscid flow, these equations led to the paradox of d'Alembert (ref. 3), that is, contrary to the situation encountered in the flow of real flow, the drag force on a solid body in a uniform flow was zero. The idea that real fluids exert some sort of friction was associated with the concept of viscosity, for which Newton (ref. 4) had presented a crude model. In the nineteenth century, the main theoretical motivation was to provide scientific reasons why drag existed in a fluid at all. Great efforts were made to explain how a vanishingly small frictional force in the fluid can have a significant effect on the flow properties. Navier (ref. 5), Poisson (ref. 6), St. Venant (ref. 7) and Stokes (ref. 8) provided rigorous theoretical explanations for viscosity. The paradox was that

progress in aerodynamics depended on this explanation of viscosity, but its presence complicated the mathematics so as to make the determination of drag impossible at high speeds. The mathematical difficulties of integrating the Navier-Stokes equations could be eliminated by neglecting the nonlinear terms. This approximation, valid only for slow motions, at least gave nonzero drag, but it yielded drag too small in magnitude for faster motions.

Helmholtz (ref. 9), Kirchhoff (ref. 10), and Rayleigh (ref. 11) dealt with the problem of flow separation from a sharp edge, again to reconcile real flows and inviscid theory. The mathematical model permitted free-streamlines to exist, across which the fluid characteristics change discontinuously, thus avoiding the paradox of d'Alembert. This free-streamline model led to the concept of a vortex sheet. This model was, however, of limited use because of the difficulties of predicting the shape of the vortex sheet and of determining the pressure on surfaces in the separated region.

Prandtl (ref. 12) provided a conceptual breakthrough. His idea was that for large Reynolds numbers, the effect of viscosity is confined to a thin layer of fluid adjacent to a solid surface. In this layer, a rapid change from virtually inviscid flow to viscous flow takes place. In this transitional (ref. 13) or boundary-layer region, an approximate form of Navier-Stokes equations may be used; outside this region, the Euler equations apply. The small thickness of the boundary layer simplifies the Navier-Stokes equations to the Prandtl boundary-layer equations. Using these boundary-layer equations on a flat plate, Blasius (ref. 14) was able to deduce a law for the laminar skin friction that agreed with the experimental data.

The boundary-layer concept, originally developed for laminar, incompressible flow along a solid boundary, has been extended to the corresponding cases of turbulent, incompressible flow, compressible flow, and also to boundary-free shear flow occurring in wakes and jets. This concept, having changed the type of the governing equation from elliptic form to parabolic, and reduced its order in the streamwise direction, sometimes gave rise to difficulties when attempts were made to improve on it, because a systematic approach of improvement was lacking. Stüper (ref. 15) first accounted for the effect of displacement thickness to improve the boundary-layer solution of flow past an airfoil. But a systematic approach, called the method of matched asymptotic expansions, was only developed much later (ref. 16). Improvements in boundary-layer solutions were found only for flows without separation. Further, the evolution of three-dimensional boundary layers under a prescribed external velocity field is still imperfectly understood (ref. 17).

A consequence of the boundary-layer concept is that when the skin-friction coefficient vanishes, the boundary layer no longer has only a small effect on the inviscid flow outside. Prandtl introduced the phrase "flow separation" to describe the phenomenon of the inviscid flow leaving the neighborhood of the surface in an adverse pressure gradient. Goldstein (ref. 18) showed that the solution of the boundary-layer equations could not be continued downstream of separation. Whenever the external velocity (or pressure) is prescribed, a singularity arises in the boundary-layer calculations. A two-layer model of the boundary layer was proposed by Lighthill (ref. 19) and, according to Stewartson (ref. 17), independently by Müller (ref. 20) to overcome

the impasse caused by this separation singularity. Further, it was shown by Lees and Reeves (ref. 21) and by Catherall and Mangler (ref. 22) that it is possible to construct external velocity distributions that do not lead to the singularity. These studies culminated into the formulation of the localized theory of the triple-deck developed independently by Neiland (ref. 23), Stewartson (ref. 24) (see also Stewartson and Williams, ref. 25), and Messiter (ref. 26). During the 1970s considerable progress was made in further development and application of this theory for two-dimensional flows, particularly for laminar flows (ref. 17). The development of a rational theory for three-dimensional, and possibly unsteady two-dimensional flows, is considered to be in its infancy. Further, the limiting form of the structure of turbulent separation and of a large separated region has not been developed.

In the past, aerodynamicists were primarily interested in aircraft and airship-like shapes and were interested in streamline shapes that prevented or limited separation (ref. 27). In the cruise condition, this is still the aim for aircraft of moderate-to-high aspect ratio. But at present, there are significant other applications in which effects of controlled separation and vortex flows are incorporated in design of aircraft.

The importance of unsteady aerodynamics in helping with an understanding of aircraft stability was recognized during the First World War (ref. 28). Flutter, an important problem caused by the interaction of aerodynamics and structural design, was identified. There was interest in how the circulation grew or was modified as an airfoil was started from rest, or changed its incidence quickly. Further, Farren (ref. 29) studied the dynamic stall of a pitching airfoil, a phenomenon of importance in the design of helicopter rotors.

Future Emphasis

Increasingly, there is a need to understand and predict the phenomenon of flow separation, of vortex flow, and of flow unsteadiness, because there are numerous present applications in which such phenomena exist. A better understanding of these phenomena may result in new applications.

Three-dimensional regions of separation generally exist on aerodynamic and underwater hydrodynamic configurations. Some examples from aerodynamics are the following. On an aircraft of moderate-to-high aspect ratio, at high lift and low speeds (for example, in the landing mode), there could be substantial regions of separation. Controlled separation from sharp edges is the hallmark of low-aspect-ratio wings. Controlled vortex flow can be used to clean up a detrimental separated flow, as for example, the vortex flow from a strake on a low-aspect-ratio aircraft. Further, the requirement for high rates of turning by military aircraft and missiles precludes maintenance of attached flows on smooth surfaces. Inviscid theory cannot determine the location at which a three-dimensional boundary layer detaches from the surface and forms a well-organized vortex. This requires a viscous theory.

There are many situations in which time-dependent aspects can be neglected. But, in a sense, it is steady flow that is peculiar. Fundamental understanding of the

nature of transition from laminar to turbulent flow and of the detailed characteristics of turbulent flows requires study of unsteady flows. Practical areas in which unsteady phenomena predominate are increasing and will continue to increase significantly. Generally, separated flows and vortical flows are inherently time-dependent.

Unsteady aerodynamics is no longer a topic of limited applications (ref. 30). For example, the structural dynamics of a helicopter rotor interact with unsteady aerodynamic aspects that are manifested during the forward motion of the helicopter. The flow over each blade is greatly influenced by a very complex wake shed from the other blades. There are three-dimensional unsteady transonic effects on the advancing blade and, generally, dynamic stall phenomena on the retreating blade. This helicopter rotor problem is somewhat analogous to the aerodynamics of flight in a gusty atmosphere. Shock waves that terminate in the vicinity of boundary layers are seldom steady, particularly at transonic speeds; see, for example, references 31 and 32. Flutter prediction and prevention (refs. 33-35) and the stability of aircraft and missiles depend on the unsteady interactions between largely viscous-oriented aerodynamics and structural dynamics. The elimination of buffet, stall, and to some extent control-surface buzz depends on unsteady viscous effects. The evaluation of heat transfer to the stagnation region of a blunt body executing oscillations in pitch is an example of an unsteady boundary-layer problem. In turbomachines, unsteady effects are important in determining performance, blade flutter, stall surge, and system response to inlet distortions (refs. 30, 36-38). The reduction in aerodynamic noise, in part, depends on the dissipation of acoustic energy by viscosity (ref. 39); this requires the study of wave motions in fluids.

There are other areas of fluid dynamics which contain unsteady viscous effects. For example, industrial aerodynamics is concerned with the oscillatory lift and drag forces that accompany unsteady separation and vortex shedding from bluff bodies such as buildings, bridges, and automobiles. Problems in hydrodynamics are somewhat analogous to those in aerodynamics (ref. 40). In hemodynamics, the flow of blood downstream of constrictions and at branching junctions of the aorta and the large arteries also exhibits the phenomena of unsteady separation and vortex shedding (ref. 41).

Birkhoff has observed that it was the development of aerodynamics that gave fluid mechanics its current, more technical and empirical orientation (ref. 42). This trend is likely to continue, although aerodynamics primarily deals with momentum transfer rather than heat or mass transfer and, although for aerodynamics, fluid viscosity cannot be neglected as it can be in some other applications. The current and future aerodynamic design needs are no different from those in the past: airframe efficiency, control, and maneuverability. But, future emphasis is likely to be on determining effects of viscosity as it affects drag, flow separation, vortex flows, and unsteady flows. This emphasis will lead to new developments in aerodynamics and, consequently, in fluid mechanics.

The effects of viscosity on nonboundary-layer types of fluid flow were studied in the past largely indirectly. For example, a separation bubble is often implied from the measurements of surface-pressure distribution. Presently, viscosity effects are studied

both directly, through computational fluid dynamics and advances in experimental techniques, and indirectly through experimental techniques. Future computers will allow these effects to be studied more directly, primarily, via computational fluid dynamics; however, experiments will always be needed to verify both computational and theoretical aerodynamics, and to provide answers when these disciplines cannot. It has been observed by Rogers (ref. 43) that most of the progress in theoretical aerodynamics has been already made. Further conceptual progress in theoretical fluid dynamics will be made, as in understanding the nature of turbulence. Like experiments, theoretical fluid dynamics will support and check computational fluid dynamics. However, one of the dominant themes in fluid dynamics during the lifetime of a future research worker born at the time of this writing will be computational fluid dynamics. Although it is likely to provide the most new knowledge, for example, in aerodynamics, the computational tasks in front of him are very difficult.

Scope

The basic equations governing viscous fluid motion are essentially nonlinear (more precisely, quasi-linear) and coupled, and therefore, exact (analytical) solutions are rare. The only recourse available is to solve the equations for a physical problem by a numerical procedure, a process which is approximate and time-consuming. In this process, it is, therefore, necessary (1) to determine the appropriate governing equations, including a model for turbulence; (2) to determine the computational form of these equations, the scaling laws, and the coordinate system; and (3) to choose the computational methods, space-time grid systems, and accuracy requirements. To achieve all this, it is imperative that the flow regimes and scales of fluid motion be identified. Primarily, the flow regimes are characterized by the relative magnitude of various terms in the equations of motion and flow parameters. The scales of motion are evaluated by experimental observations or by assumptions (or conjectures) when there is no experimental information. These are spatial scales and temporal scales that generally differ in different parts of the flow field. Along with the study of a kinematic property of flow of fluids, namely, vorticity, the flow regimes and scales of motion also provide an understanding of flow structure.

The discussion of physical aspects starts with a brief identification of some of the flow regimes. This is followed by a discussion of scales of motion, both spatial and temporal. This article is concluded with a brief indication of the importance of vorticity and a description of how the vorticity is generated.

It is intended that this article be a broad reference work on physical aspects of computing the flow of a viscous fluid. Because the subject is vast, an attempt is made to identify and briefly describe these aspects rather than to provide a self-help encyclopedia.

FLOW REGIMES

The classification scheme considered here for viscous-flow regimes is primarily a series of binary subclassifications (fig. 1). These are the following: (1) incompressible and compressible, (2) steady and unsteady, (3) laminar and turbulent, (4) attached and separated flows, (5) Navier-Stokes and non-Navier-Stokes, (6) weak and strong shock/boundary-layer interactions, and (7) simple and complex strain fields. The first four classifications may be considered as based on physical aspects and the rest may be considered as based on analytical aspects. There are also intermediate regimes such as transitional, subsonic, transonic, supersonic, and hypersonic flows. Most of these are standard and well known. We shall comment on computationally significant physical aspects of most of these flow regimes.

Conditions of Incompressibility

The classical Navier-Stokes equations are applicable, when the following assumptions are valid. First, when the velocity distribution is approximately solenoidal. In other words, when the changes in density of a material element resulting from pressure variations are negligible. (This is, strictly speaking, the condition of incompressibility.) The density variations are negligible in the absence of body forces when (1) the Mach number, M_∞ , is less than about 0.3 everywhere in the flow field, and (2) when the flow

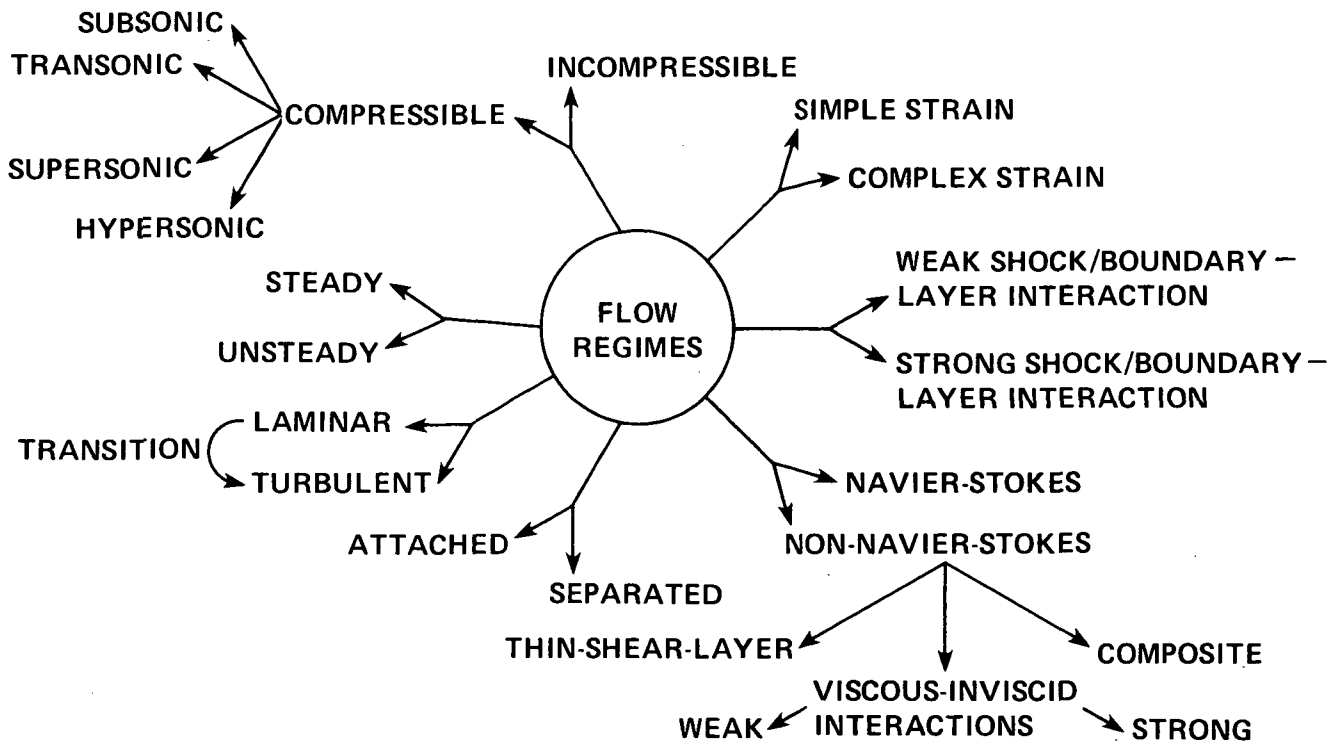


Figure 1. - Classification scheme for viscous-flow regimes.

is slowly varying, that is, when the product of the dominant frequency of unsteadiness and characteristic length scale is much smaller than the speed of sound. Second, when the viscosity is constant. Third, when the thermodynamic processes of the fluid are irrelevant. (That is, when the heat added by dissipation and conduction is negligible, and when the enthalpy changes are negligible owing to pressure variations.) Therefore, when the temperature differences in the flow are not large, the heat-transfer problem can be treated separately or in parallel with the flow problem. In compressible flows, these two problems are intimately interconnected.

Transitional Flows

The phenomenon of transition from laminar to turbulent flow in vortical two- or three-dimensional, external-, internal- or free-shear layers has so far eluded the completely rational understanding that is needed in predicting practical applications (refs. 44-46). Reynolds (ref. 47) and later Rayleigh (ref. 48) hypothesized that transition to turbulent flow is a consequence of the instability of the laminar flow. When vorticity, entropy, and sound disturbances penetrate a laminar shear layer, they initiate in it forced and free response (fig. 2). If these initiating disturbances are large, they grow by the forcing mechanism to (three-dimensional) nonlinear levels and lead to a turbulent shear layer, as explained below. This is the high-intensity bypass process (ref. 44). If

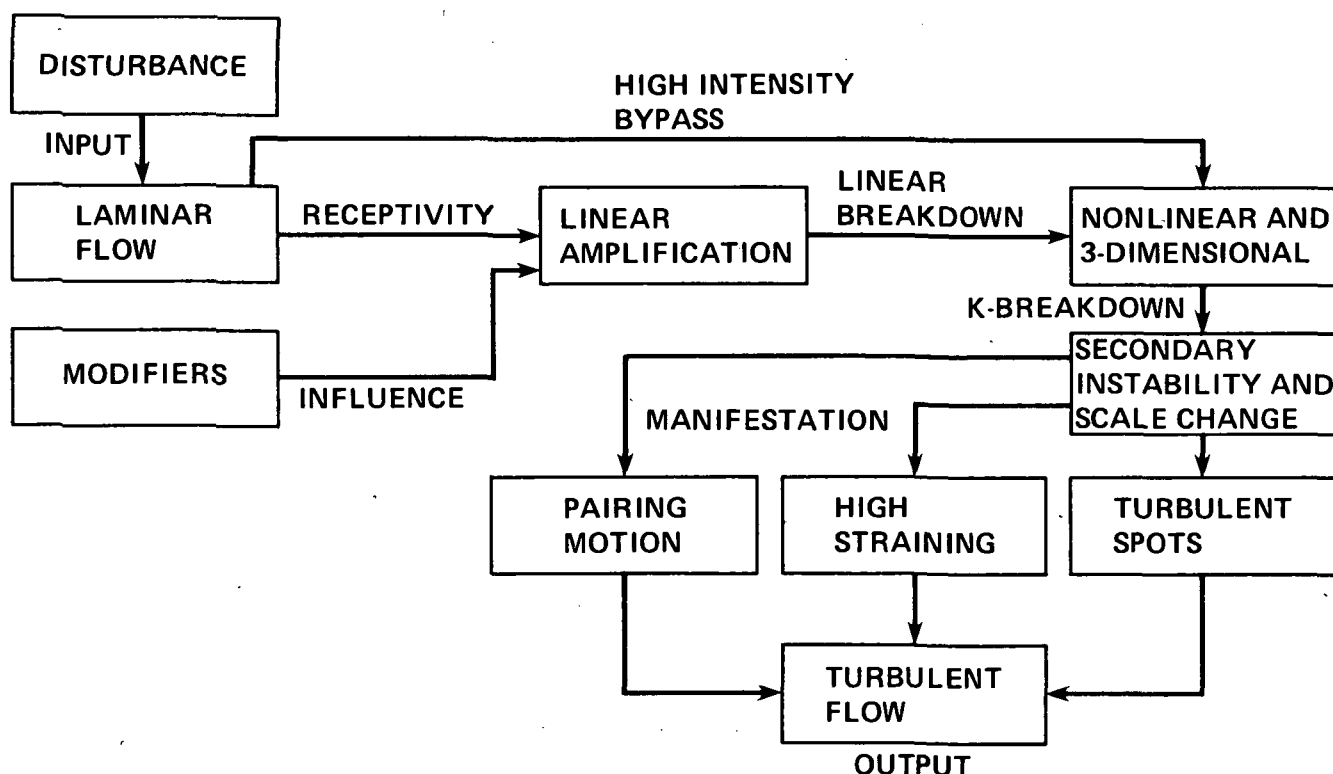


Figure 2. - Many facets of the laminar-turbulent transition process
(based on refs. 44 and 46).

they are small, they excite and linearly amplify free disturbances (such as, Tollmien-Schlichting (TS) waves or Görtler waves) in the laminar shear layers. This receptivity of shear layers to small disturbances is influenced by "operation modifiers" such as pressure gradient, curvature, surface waviness, roughness and temperature, angle of attack, angle of yaw, leading-edge sweep, Mach number, suction, and blowing. The TS waves amplify and cease to follow the predictions of the linearized theory, and three-dimensionality of flow motion and vorticity stretching emerge. The initialization of three-dimensional, high frequencies associated with secondary instabilities and characterized by a sudden spike in the streamwise velocity signal is called the K-breakdown (ref. 46) of laminar flow. Subsequently, turbulent spots are formed in external and internal shear layers, high straining is produced in rotating flows, and pairing motion of rolled-up vortices is observed in free-shear layers. Growth of these flow features leads to turbulent shear layers. It is viscosity which limits the growth of disturbances. This process of transition from laminar to turbulent flow is not a well-defined problem because of the sensitivity to poorly defined initiating disturbances. An example of a transitional flow is the leading-edge separation bubble, sometimes, observed on airfoils and illustrated in figure 3.

The only tool that can provide information, unobtainable from experiments and theory, to the nonlinear-laminar-to-turbulent transition process is the numerical solution of the compressible Navier-Stokes equations. The main requirements are that (1) the discretization errors do not contaminate physical phenomena such as instabilities, that is, the finest scales in the transition process are adequately resolved in space and time; and (2) the introduction of artificial boundaries owing to the limited size of the computational domain does not interfere with the physical upstream influence, the ellipticity of the Navier-Stokes equations.

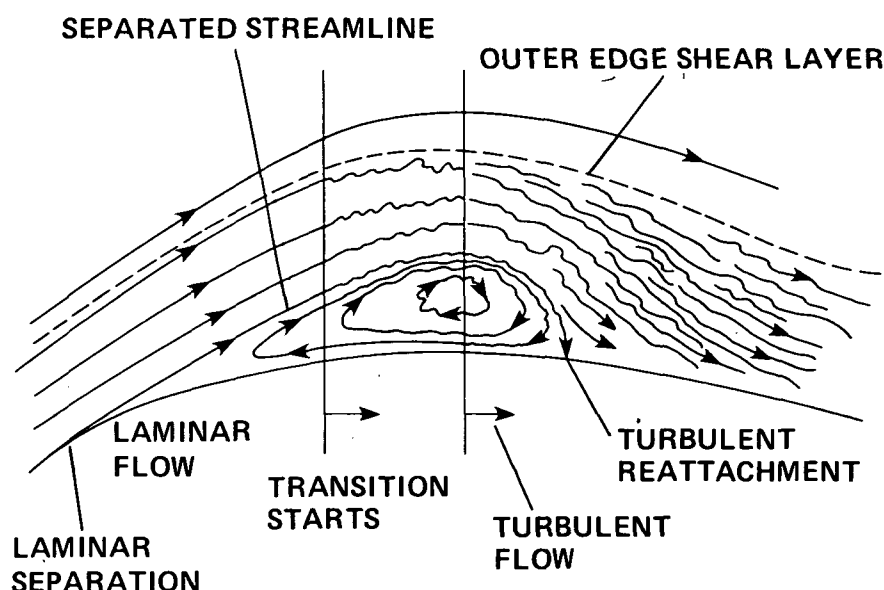


Figure 3. - Transition in a free (separated) shear layer (transitional separation bubble).

Turbulent Flows

As in the case of the transition simulations, the direct turbulence simulations represent an attempt to resolve all scales of motion accurately both in time and space. This means that the only errors made are numerical ones, and there is no need for turbulence modeling. The principal problems are to encompass a broad enough range of scale and to compute a large enough sample so that the simulated event is meaningful. Computer resources limit such simulations to much-lower-than-normal Reynolds numbers and to unbounded, homogeneous, and inhomogeneous turbulent flows.

At normal (high) Reynolds numbers, viscosity plays a small part in the behavior of turbulence, except in the viscous sublayer and superlayer of a turbulent boundary layer (fig. 4). Generally, large-scale motions dominate transport processes and small-scale structures dissipate energy by the action of viscosity. The large-scale structures are not universal. Except possibly in flows with strain or shear (ref. 49) (the flows of aerodynamic interest), the small-scale structures are nearly universal or isotropic at very high Reynolds numbers and the spectrum of small-scale fluctuations can be parameterized by the local rate of energy dissipation and the kinematic viscosity. This spectral behavior leads to the concept of so-called large-eddy simulation (LES)¹ where

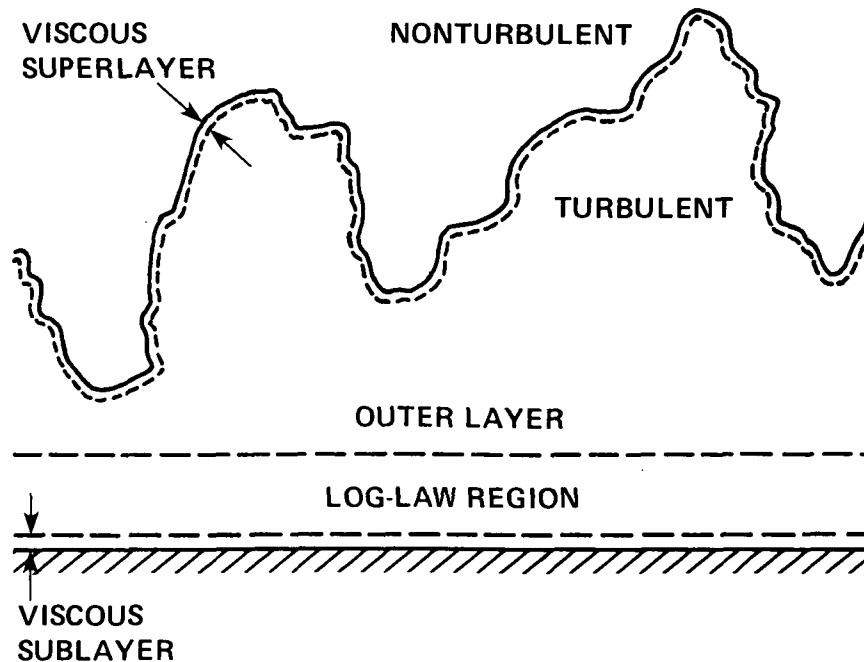


Figure 4. - Sketch of instantaneous turbulent boundary layer and defined statistical regions.

¹The adjective "large" is misleading when the important scales to be resolved are also small as, for example, near solid surfaces. Further, the word "eddy" is also a misnomer when the simulation is not in a spectral space, as it is a statistical concept of Townsend (ref. 50) describing the stochastic picture of turbulent fluid through the Eulerian spatial-correlation tensor, not a physical structural descriptor.

the larger eddies are computed directly and the very small eddies are modeled. This idea originated in the works of Smagorinsky (ref. 51), Lilly (ref. 52) and Deardorff (refs. 53-55); the Stanford-Ames LES program further developed it, providing extensive demonstrations (see for example, refs. 49, 56-60).

In the LES approach one derives equations for the grid-resolvable field from the Navier-Stokes equations by averaging over spatial grid-volumes. These equations involve terms associated with the grid-unresolvable structures, which have to be modeled. By definition, turbulence is necessarily unsteady and three-dimensional, and, therefore, in this approach time-dependent and three-dimensional computations are necessary. Modeling of scales, which are not resolved by the grid system, is done by phenomenological models of the simple eddy-viscosity type when the small-scale structures are homogeneous and isotropic. These models seem to be inadequate for inhomogeneous flows (ref. 55). In addition, in regions in which viscous effects are important, these models are less likely to be satisfactory. In such cases, complex modeling, for example, equations for Reynolds stresses, may be required. The degree of complexity of modeling turbulence is essentially the same whether the averaging is done over spatial dimensions or over the time dimension, provided the computations are done in three dimensions and in a unsteady mode.

The LES approach is in its infancy for computations of viscous flows. At present the approach has been limited to fully developed turbulent flows, to incompressible fluids, and to periodic boundary conditions in the streamwise and spanwise directions, that is, to extremely simple flow fields. The only flow that has been extensively studied is the channel flow (refs. 54, 59, 61-64). The computations of the turbulence field in practical applications almost always are done with the time-averaged equations of motion.

Navier-Stokes Regime

When a shear layer is not thin or slender (fig. 5), the Navier-stokes equations are necessary. (A variation of velocity in the direction normal to the direction of the velocity itself is called a rate of shear strain. The region over which this variation takes place is called a shear layer.) The upstream influence of both the pressure field and streamwise gradients of viscous and turbulent stresses are then important. The upstream influence of the pressure field is much more pronounced than in a thin-shear layer owing to significant normal pressure gradients; for example, in large separated regions, in the trailing-edge region of an airfoil and in interactions of a shock wave and a boundary layer. Further, the streamwise gradients of stresses cannot be neglected (1) in low-Reynolds-number flows; (2) when the velocity field encounters rapid variations in streamwise direction, such as past the trailing edge of an airfoil, across a shock wave within a boundary layer, and around a point of flow separation; (3) when transition or turbulence is computed without modeling it; and (4) when viscous LES simulations are done.

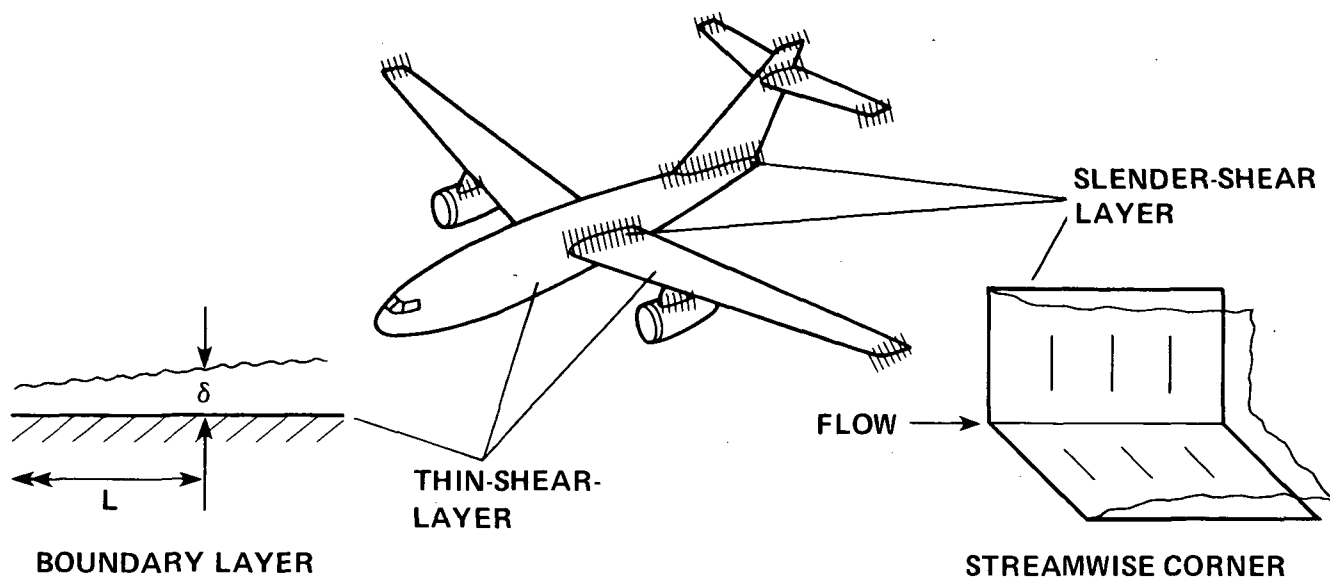


Figure 5. - Thin-shear layers and slender shear layers (shaded) on a commercial transport plane in a cruise condition.

Non-Navier-Stokes Regime

The subclassification of viscous flow regimes in terms of non-Navier-Stokes and Navier-Stokes is based on the form of governing equations that are used to compute the flow fields. In the former category, we have (1) the thin-shear-layer theory (ref. 65), (2) the strong viscous-inviscid interaction theory, and (3) the composite theory. The first is traditionally known as the boundary-layer theory. It includes both the classical and higher-order formulations. The second includes theories such as the interacting boundary-layer theory (ref. 66) and the triple-deck theory or the asymptotic theory of free interactions (ref. 67). The last includes the composite thin- and slender-shear-layer theory; and it contains the parabolized Navier-Stokes theory.

Thin-shear-layer theory - In the absence of flow separation (that is, departure of the shear layer from a solid surface), a steady, asymptotic solution of the Navier-Stokes equation at large Reynolds number is determined from the classical boundary layer theory. This solution is the first approximation to the solution of the Navier-Stokes equations. The second-order corrections can be classified into two categories, according to the appearance of curvature terms in the differential equations or through the interaction with the flow external to the boundary layer. It is convenient to subdivide each of these categories further. Curvature effects are due to longitudinal or transverse curvature or both. In incompressible fluids, the interaction effects are due to displacement by the wall-bounded viscous layer of the external flow, the external vorticity, and the external gradient of the stagnation temperature. In compressible fluids, the interaction effects result from displacement of the external flow, external gradient of entropy, and the external gradient of enthalpy. A further classification arises in this case, namely, effects caused by noncontinuum surface phenomena (ref. 16).

The boundary-layer theory is the most developed for laminar flows, for steady motions, and for plane or axisymmetric flows. Although the classical boundary-layer equations are nonlinear, all equations of higher-order corrections are linear; consequently, the above second-order corrections are additive.

The boundary-layer theory is based on the assumption that the shear layer is thin and on the condition that this layer grows only slowly in the general direction of flow. This theory is applicable not only to layers on a boundary but also to layers in jets and wakes. Therefore, it is also called the thin-shear-layer theory. As a consequence of the above assumption and condition, the upstream influence within the thin layer is not accounted for by the first-order theory and is only partially accounted for by the second-order theory. This is the fundamental limitation of the thin-shear-layer theory.

The upstream influence is provided by the pressure field in subsonic regions, by transport of momentum in the upstream direction in separated flows, and by streamwise gradients of viscous and turbulence stresses, as indicated by the direction of arrows in figure 6. The first or the last of these influences makes the flow field and the governing equations elliptic in the spatial dimensions. The correction owing to the displacement effect can indirectly transmit the upstream influence of the pressure field via the external flow, but not through the shear layer. A correction owing to displacement thickness in the "inviscid" flow at a station leads to a correction in the pressure distribution upstream of this station. This procedure is a part of the viscous-inviscid interaction theory. On the other hand, the correction owing to curvature effect accounts for the variation of the pressure field across the shear layer, but not for the upstream influence of this field through this layer. In addition, this correction is limited to shear layers that are thin, since the curvature of streamline varies substantially across thick-shear-layers. The upstream influence of the velocity field can be numerically accounted for by methods, such as the DUIT scheme (ref. 68), which march both upstream and downstream alternately. However, these methods are limited to flows

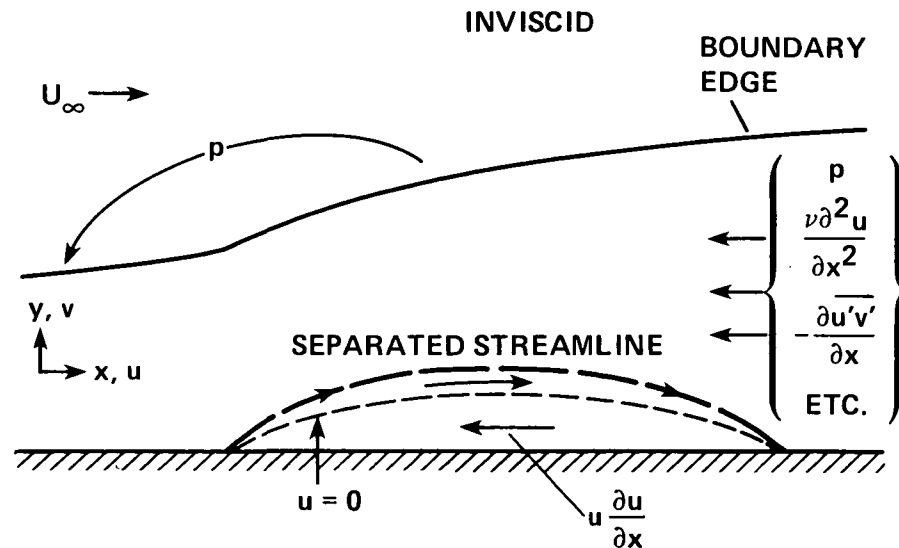


Figure 6. - Upstream influence of pressure field (p), transport of momentum in separated flows, and streamwise gradients of viscous and turbulent stresses (boundary-layer growth is exaggerated).

in which there is significant upstream influence of the velocity field relative to that of the pressure field within the shear layer so that the latter can be neglected. This is usually the case in high- Re , laminar separated flows. The thin-shear-layer theory does not account for the upstream influence of streamwise gradients of viscous and turbulence stresses. These stresses are generally negligible at normal (high) Reynolds numbers. In a shock wave, the viscous diffusion is not negligible (provided the Navier-Stokes equations are valid, see the discussion of thickness of shock waves in the section entitled Spatial and Temporal Scales), and in a shock layer formed by the interaction of the shock wave with a shear layer, both viscous and turbulent streamwise diffusion may be significant.

The thin-shear-layer equations are singular when the normal momentum (or the error in conserving it) is not negligible. In a steady flow for an incompressible fluid, this singularity occurs at the location where the flow separates. At a singular point or a line, the direct (pressure-specified) computational procedures fail; but the inverse (displacement-thickness or wall-shear specified) procedures usually work, when the upstream influence of the pressure field is negligible compared to that of the velocity field. The inverse procedures simply ignore the significant upstream influence of the pressure through the shear layer at and in the vicinity of the separation location (see also refs. 69 and 70).

A further discussion of the thin-shear-layer theory was recently given by Telionis (ref. 71).

Viscous-inviscid interaction theory - If different regions of a flow field can be studied almost independently with good approximation, these regions are said to have a weak interaction. When the different regions cannot be treated separately because of strong coupling, the flow is classified as one with a strong interaction. This is explained again by considering the displacement effect of a viscous layer on the inviscid flow. (The words "viscous" and "inviscid," respectively, stand for having significant and negligible viscous-stress terms and turbulent-stress terms.) First, the inviscid pressure distribution is determined independent of the viscous layer. This first inviscid approximation is used to obtain the first viscous approximate solution. Then the second inviscid approximation is computed taking into account the displacement effect caused by the viscous region resulting in the second inviscid pressure distribution. This in turn is used to determine the second approximate solution of viscous region. If the second approximate displacement surface is practically the same as the first one, then this iterative procedure is stopped, and the viscous-inviscid interaction is commonly known as a weak interaction (see, for instance, (refs. 72 and 73). If however, the iterative procedure must be repeated a large number of times, then the interaction is considered to be strong.

The thin-shear-layer theory fails when there are nonuniformities or abrupt changes in the surface boundary conditions caused by flow separation, by a corner, by strong injection, by a trailing edge, or by a shock wave intersecting the boundary layer. In the neighborhood of such nonuniformities, the normal pressure gradients will be significant. For example, once laminar flow separates, it may not be possible to use the irrotational inviscid solution as a basis for determining a uniformly valid first approximation to

the flow as Re tends to infinity. Flow separation that occurs in an adverse pressure gradient is accompanied by sharp increase in displacement thickness. This dramatic change in the boundary-layer structure has a significant effect on the external flow. During this interaction of the boundary layer and the inviscid flow, the viscous effects are confined to the lower part of the boundary layer; the rest of the boundary layer behaves virtually as if it were inviscid. These two parts of the boundary layer are usually referred to as the lower and the main decks, respectively (refs. 19, 20). The region of the external flow field just above the two decks is most affected by the rapid changes in these decks; it is called the upper deck (fig. 7). This multilayered structure of the boundary layer and the associated analytical procedures for laminar flows have been called the triple-deck theory (ref. 74). This theory is applicable if the streamwise length of nonuniformity is relatively short. Another example of dramatic change of the boundary-layer structure affecting the external flow is that of a weak shock wave sharply increasing the displacement thickness, even in the absence of flow separation.

The multilayered structure of a turbulent boundary layer caused by nonuniformities is different from that of a laminar boundary layer. This difference is caused by the basic difference in structure of the turbulent and laminar boundary layers. In the main deck, the viscous stress gradients are usually neglected in laminar flows, whereas the Reynolds stresses are considered frozen along the streamlines in turbulent flows. Further, the turbulent boundary layer develops a two-layer structure described by the law of the wall and the law of the wake, as formulated by Coles (ref. 75) for incompressible fluid and as modified by Maise and McDonald (ref. 76) for compressible fluids. In this case, the asymptotic theory leads to a mismatch in both the Reynolds stress and streamwise velocity between the main and inner decks (refs. 66, 67). This mismatch is resolved by introducing a "blending layer" (ref. 66) or "Reynolds-stress sublayer" (ref. 77), resulting in the "four-deck" theory. However, the nonasymptotic theory (ref. 78) does not use this blending layer. There are also qualitative differences in interactive response between laminar and turbulent flow. In the latter case, there is much smaller upstream influence of pressure, and the boundary layer is less prone to separate. Note that no model has been developed for turbulent separated flows (ref. 79).

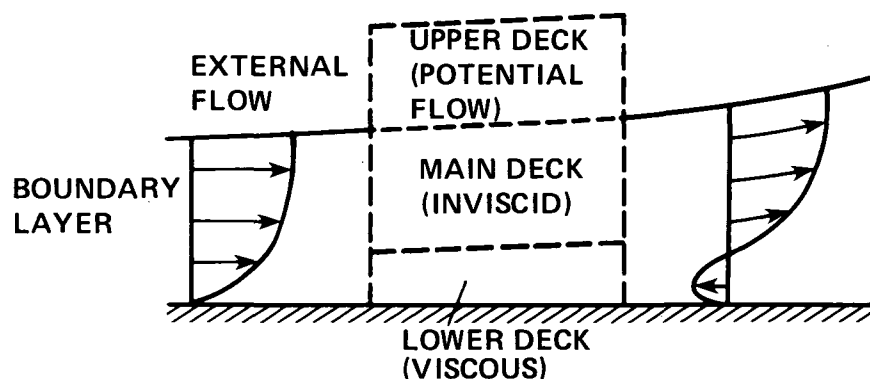


Figure 7. - Schematic of three decks in the vicinity of separation point (based on ref. 74).

Composite theory - The basic ingredient of the interaction theories, for high-Reynolds-number problems, is the coupling of the external inviscid and thin- or slender-shear-layer flows. Instead of achieving this coupling through matching boundary conditions, it can be achieved by considering a set of equations, less complex than the Navier-Stokes equations, that are valid for both these flows. The basic idea is similar to that of Oseen (ref. 80) who corrected the nonuniformity in Stokes's approximation for plane flow at low Reynolds numbers by partially including the neglected convective terms. If a set of equations includes the inviscid equations and the viscous and turbulence stress terms, for example, from the thin-shear-layer equations, which are absent in the inviscid equations, then the resulting equations automatically achieve the coupling between inviscid and viscous flows. These equations are called composite equations in singular-perturbation theory (ref. 81).

The composite equations for thin-shear-layers contain leading terms up to second-order in the viscous-inviscid interaction theory. These equations are called the composite thin-shear-layer equations². In a body-fitted or optimal (refs. 82, 83) coordinate system, a composite set of equations exhibits upstream influence of the pressure field through the shear layer, but not upstream influence of viscous and turbulent stresses. In the absence of these stresses, the parabolic form for the velocities in streamwise direction has led to the expression "parabolized Navier-Stokes equations." These equations may be used to solve problems that particularly need to be treated by the strong viscous-inviscid interaction theory. In addition, these equations are necessary for studying upstream influence of pressure field through shear layers and flow fields such as the strong-interaction region downstream of the sharp leading edge of a flat plate in hypersonic rarefied flow, a mixing region with a strong transverse pressure gradient and a blunt body in a supersonic flow at high altitudes.

Shock Waves

In the absence of viscosity, the interaction of a shock wave with a solid surface would result in a surface-pressure discontinuity and possibly an irregular reflection. In reality, viscosity makes the surface pressure continuous. The interaction of a shock wave with a boundary layer is a complex phenomenon, see, for instance, references 84-88. It can occur in the presence of an incident shock, oblique or normal, or be caused by an irregularity in surface shape. The external pressure "discontinuity" across the shock wave is transmitted through the boundary layer toward the subsonic part adjacent to the surface. This subsonic flow cannot support this discontinuity; as a result, pressure disturbances are emitted both upstream and downstream of the shock impingement, developing a gradual streamwise pressure rise at the surface, along with pressure gradients normal to the surface. The pressure rise upstream of the shock causes thickening of the boundary layer, which in turn generates compression waves

²These equations are commonly known as the thin-layer Navier-Stokes equations. It is, however, misleading to describe these equations as the thin-layer approximation of the Navier-Stokes equations, because the thin-(shear)-layer approximation of the Navier-Stokes equations gives the thin-shear-layer (boundary-layer) equations.

emanating from the sonic line toward the external flow (fig. 8). These compression waves converge and coalesce into the incident shock wave or a different external shock wave. Thus, there are both local effects, such as the smearing of "discontinuous" pressure rise and a different wave pattern in the external flow, and global effects, such as substantial thickening of the boundary layer downstream of the interaction region. If the adverse pressure gradient caused by the compression in front of the shock wave causes flow separation, then the interaction of a shock wave with a boundary layer is labeled as a strong-interaction problem. If, on the other hand, there is no shock-induced separation, the interaction is considered to be weak.

There is a pronounced difference between laminar and turbulent shock/boundary-layer interactions (refs. 89-91). The pressure rises more rapidly for turbulent than for laminar flows. The displacement thickness through the shock increases considerably less for turbulent than for laminar flows. Reynolds number has almost no effect in turbulent flows, but it has a strong effect in laminar flows. In turbulent flows, a large pressure rise is required for the flow to separate, and the separation point moves upstream more slowly as the shock wave becomes stronger. The opposite is the case in laminar flows. Also in laminar, attached flows, the spread of the surface-pressure distribution at the foot of the shock wave, strongly depends on the Reynolds number, increasing with decreasing Reynolds number.

Strain Fields

Modeling of turbulence is largely governed by strain fields, which are classified as being simple or complex (refs. 65, 92, 93). Simple shear layers have monotonic velocity profiles and nearly straight streamlines. In these layers, the only significant rate-of-strain component is the variation of streamwise velocity in the normal direction, $\partial U / \partial n$, which is of the same sign everywhere or changes sign only at an axis of symmetry. Simple strain fields are noticed in simple shear layers such as symmetric wakes and jets, and plane boundary layers (fig. 9). All other flows that are significantly affected by extra rates of strain, additional to this, are considered complex. In two-dimensional or axisymmetric flows, these extra rates of strain appear in shear layers that experience streamwise curvature, lateral divergence, bulk dilation, buoyancy, or system rotation; see for example, figure 10. This distinction among strain fields is made because extra rates of strain can have a large effect on turbulence, which in turn influences modeling of turbulence. Eddy-viscosity or mixing-length models can give good results when strain fields are simple, but not when they are complex.

SPATIAL AND TEMPORAL SCALES

In this section we present some of the spatial and temporal scales that are observed in viscous flows. Flow structures in transitional flows and in turbulent flows in the vicinity of a wall are described. The spatial scales of following physical phenomena are

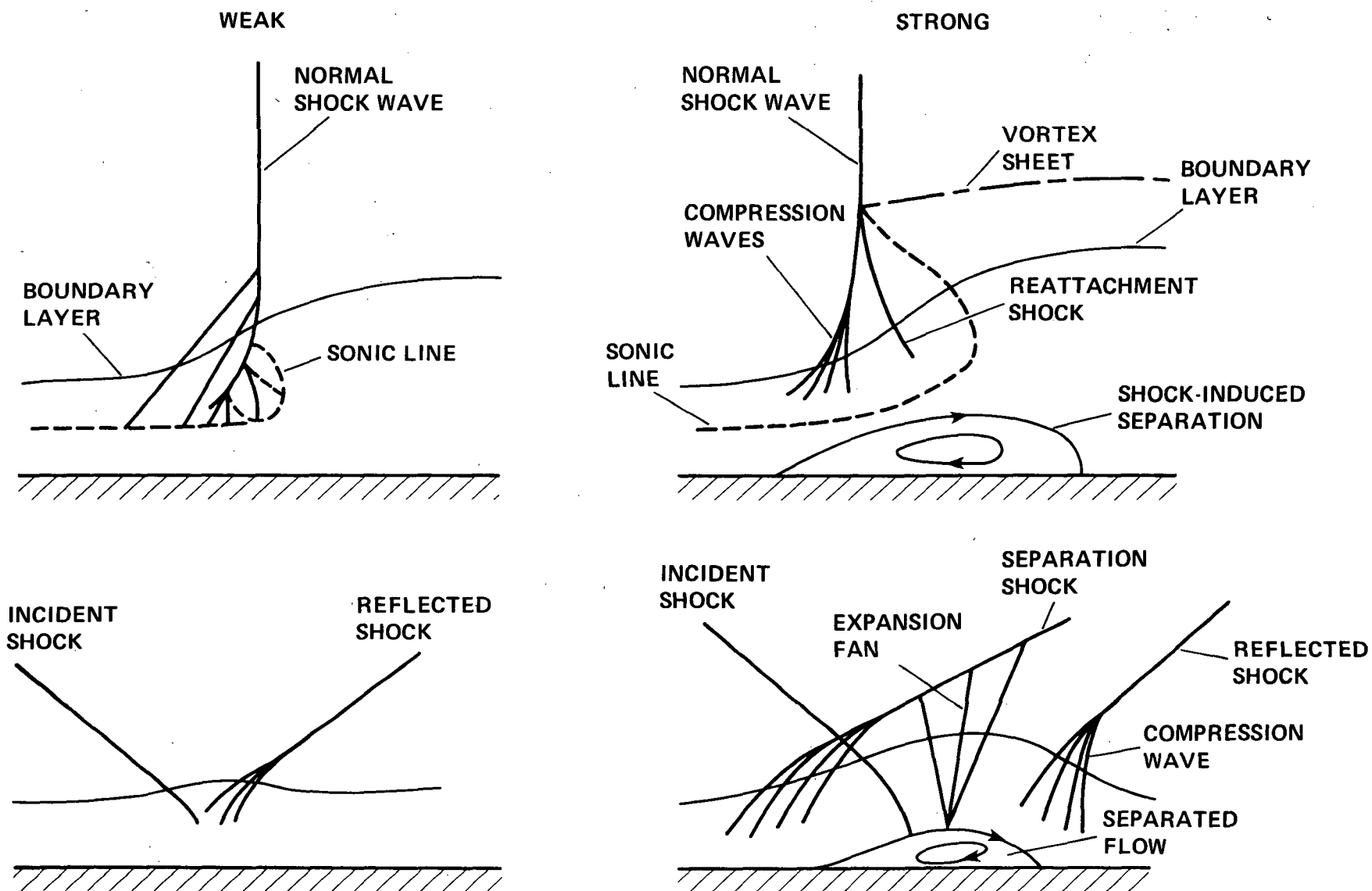


Figure 8. - Schematics of weak and strong/boundary-layer interactions.

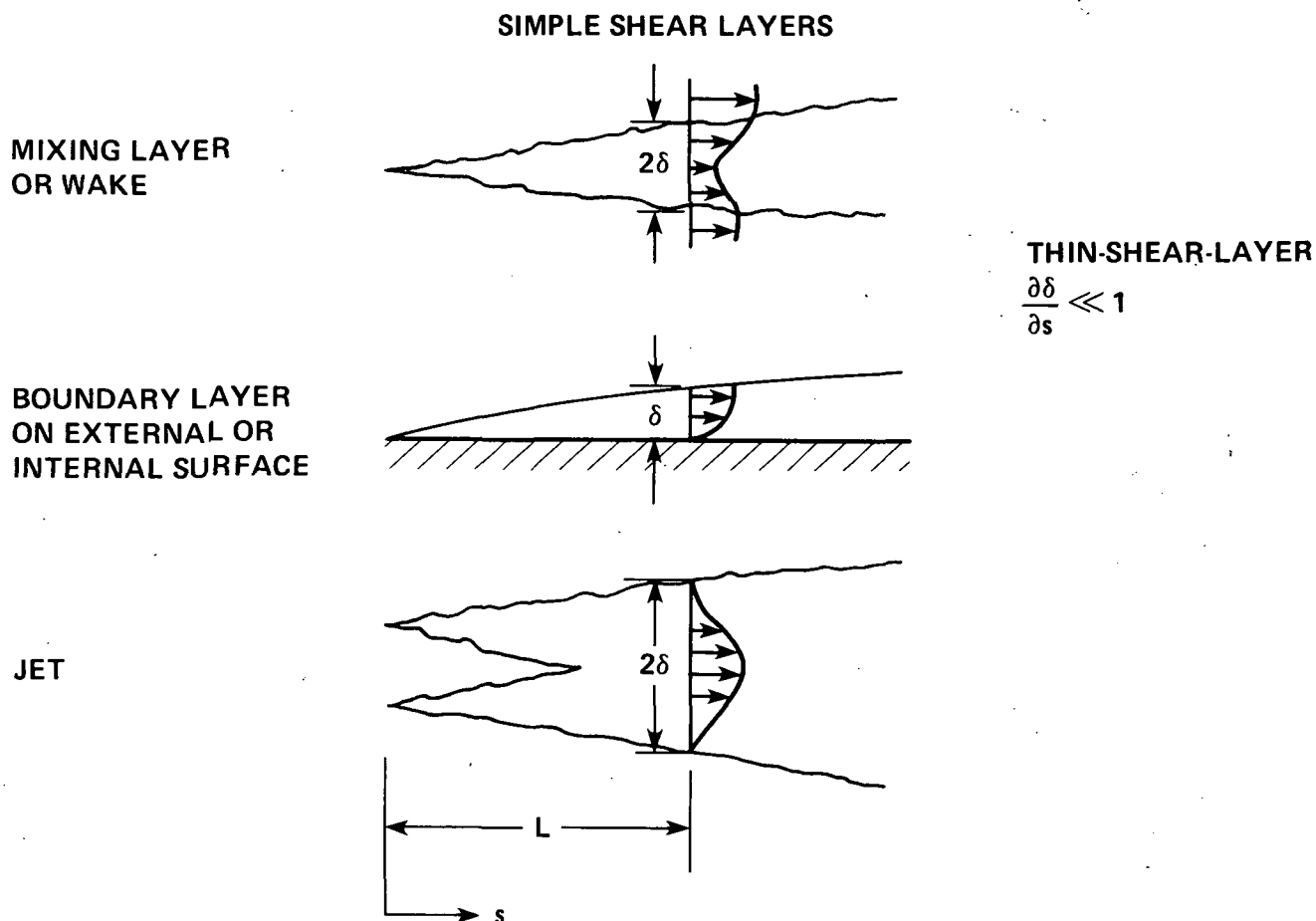


Figure 9. - Condition for a shear layer to be thin in two-dimensional or axisymmetric flows.

discussed: (1) mean turbulent boundary-layer profile, (2) thin- and slender-shear layers, (3) flow separation, flow past the trailing edge of a flat plate and weak shock-wave boundary layer interactions, (4) weak and strong viscous-inviscid interactions, and (5) shock waves. Further, based on magnitudes of strain rates, simple and complex shear layers are classified. The temporal scales are discussed in terms of the Strouhal number, diffusive time-scales, and turbulence frequencies. Primarily, these spatial and temporal scales help determine the computational space-time resolution requirements.

Flow Structures in Transitional Flows

In a transitional flow, from a laminar to a fully developed turbulent flow, the scales of motion depend on the Reynolds number of the flow and on the details of the shape of the body. Viscosity determines the relevant small scales. These scales are those in the fully-developed turbulent flow, and they are given in the next subsection.

The primary structure observed in a wall-bounded, external transitional flow is the turbulent "spot," the existence of which was first observed by Emmons (ref. 94).

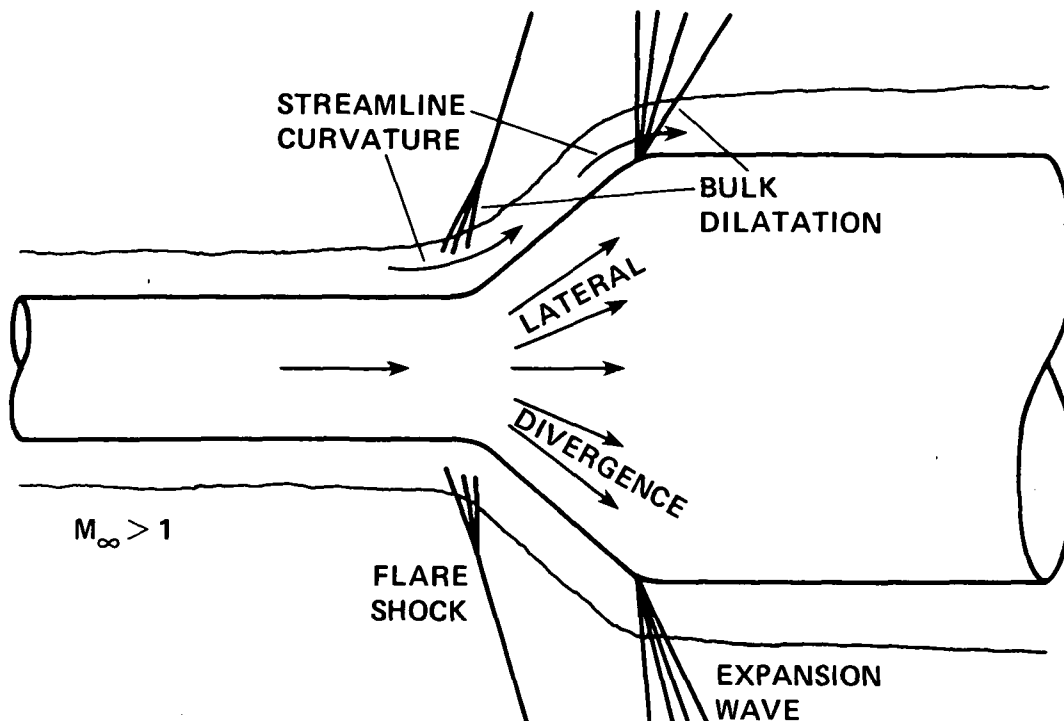


Figure 10. - Supersonic flow over a cylinder-flare with extra rates of strain produced by streamwise curvature, lateral divergence of flow, and bulk dilatation.

Each turbulent spot is surrounded by nonturbulent fluid. In plan view, it is like a rounded-off elongated delta, with blunt vertex pointing downstream (fig. 11). The upstream and downstream edges travel at constant but not equal velocities. Near the wall, the propagation speeds (celerities) of the upstream and downstream interface, are typically 0.5 and 0.9, respectively, of the free-stream velocity (ref. 95). These spot propagation velocities are larger than the velocity of the undisturbed laminar flow. Therefore, the fluid downstream of the spot is overtaken by the spot, becomes turbulent, and then again laminar after the passage of the spot. The velocity (rate) of spot growth is about 0.2 of the free-stream velocity. The motion within the spot is similar to that in a turbulent boundary layer with streamwise streaks next to the wall. The ensemble-averaged vorticities within the spot are essentially a single horseshoe vortex superimposed on small-scale motions (refs. 96, 97).

The main structure in an internal transitional flow is somewhat different from that in an external flow. For example, in a pipe a turbulent "slug" is observed. It is different from a turbulent spot. The turbulent slugs occur in smooth or slightly disturbed inlets for $Re > 3200$ based on the diameter of the pipe (ref. 98). These structures occupy the entire cross section of the pipe, and they are elongated in the streamwise direction. The leading edge and the trailing edge of the slugs travel at the same speed, relative to the maximum turbulent velocity in the pipe, as the celerities of edges in the case of turbulent spots. Another type of intermittent turbulent flow, referred to as a "puff" is also found in pipes. A turbulent puff occurs when a large disturbance is introduced

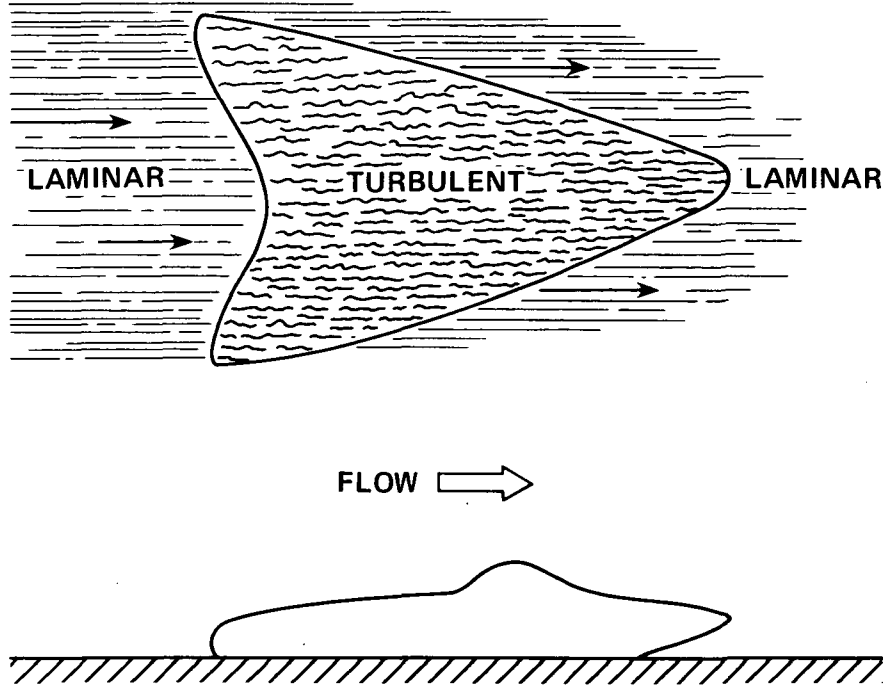


Figure 11. - Sketch of a turbulent spot.

at the entrance of the pipe for $2000 \leq Re \leq 2700$. Puffs correspond to an incomplete relaminarization process.

Scales in Turbulent Flows

Inside the viscous sublayer, the large scales are the friction velocity, u_τ , and the length scale determined by ν/u_τ , where u_τ is given by $(\tau_w/\rho)^{1/2}$. Here τ_w is the shear at the wall, and ν is the kinematic viscosity. Outside the viscous sublayer, the large scales are the fluctuating velocity relative to the mean flow, u' , and the length scale is given by u'^3/ϵ , where ϵ is the mean dissipation rate (ref. 99). Inside and outside the viscous sublayer, the small length scales are identified with the Kolmogorov microscale of length (η) determined by $(\nu^3/\epsilon)^{1/4}$, and the corresponding Kolmogorov scales of time and velocity. Actually, there is significant flow structure that is smaller than this microscale of length, both outside and inside the sublayer.

If L is a macroscopic length scale, then outside and inside the viscous sublayer, we have respectively, $L/\eta = R_\lambda^{3/2}/15^{3/4}$ and $L/\eta = O(R_\lambda^{-1/2})$, where R_λ is a Reynolds number based on the Taylor microscale ($\lambda^2 = 15\nu u'^2/\epsilon$) and fluctuating velocity relative to the mean flow. In terms of Re , the former ratio is $O(Re^{3/4})$. The Kolmogorov microscale of time is $\tau = (\nu/\epsilon)^{1/2}$, and the frequencies corresponding to macroscales are of $O(U/L)$, where U is the mean velocity. This gives $\tau/\tau \sim Re^{-(1/2)}$ where $\tau \sim L/U$. Therefore, the total number of degrees of freedom in a volume of fluid of $O(L^3)$ is $O(Re^{9/4})$.

Organized Structures in Wall-Bounded Turbulent Flows

Townsend (ref. 50) was the first to identify organized³ structures in turbulent flows. He described "double structure" of fully developed turbulence consisting of more or less organized large eddies, containing of the order of one-fifth of the total turbulent energy in an essentially unorganized, small-scale background turbulence. The concept of an eddy is a mathematical abstraction useful in constructing simplified models of turbulence. During the last two decades, there has been interest in organized structures, which somewhat differ from large eddies. These structures are identified, usually, by flow-visualization, conditional-sampling, and the Eulerian space-time correlation methods (ref. 101). Recently identification has been attempted by a technique based on conventional statistical approaches using the proper orthogonal decomposition theorem of probability theory (ref. 102). It appears that there is some form of organized structure present in all types of turbulent shear flows. However, in general, these structures contain a small part of the total energy and play a secondary role in controlling transport (ref. 102). A comprehensive review of "coherent" structures in turbulent shear flows has been recently given by Hussain (ref. 103).

Although there is a lack of consensus at present concerning the organized structures in a turbulent boundary layer, the definitions or identifications, and the physical dimensions and origins, certain characteristics of these structures are beginning to be established. These structures and their scales are relevant in any unsteady, three-dimensional computation in which most of the scales of turbulence are resolved with appropriate space-time grid, whether it uses finite space-averaging or short time-averaging.

It appears that there are five main parts of the turbulent boundary layer (fig. 12): streamwise vortices and streaks next to the wall, pockets of energetic fluid near the wall, large-scale motions in the main (or outer) part of boundary layer, mushroom-shaped intermediate-scale motions of energetic fluid near both outer and inner edge of outer-region of the boundary layer and the viscous "superlayer." The outer-region exists for $y^+ > 100$, where $y^+ = u_\tau y / \nu$ which is a Reynolds number related to the energy-containing turbulence. (Any variable, which is given the plus sign superscript, has been made dimensionless in this way, and is said to be in "wall units.") In the following paragraphs, these structures are briefly identified for a simple boundary layer, that is, in the absence of streamwise curvature, pressure gradient and roughness. Further review of these structures can be found in references 104-108.

Next to the wall, the flow structure consists of a fluctuating array of counter-rotating vortices (ref. 109) and of an alternating array of high- and low-speed regions called streaks, both aligned in the streamwise direction (fig. 13). Streaks are found in the regions between vortices. High-speed fluid moving from the outer region into the region next to the wall, called a sweep, and low-speed fluid moving out of this region,

³Organized structures are also known as coherent structures. Coherent means having the quality of cohering, of being logically consistent, or having a definite phase relationship (ref. 100). Since organized flow structures are not necessarily coherent, they are not called here coherent structures.

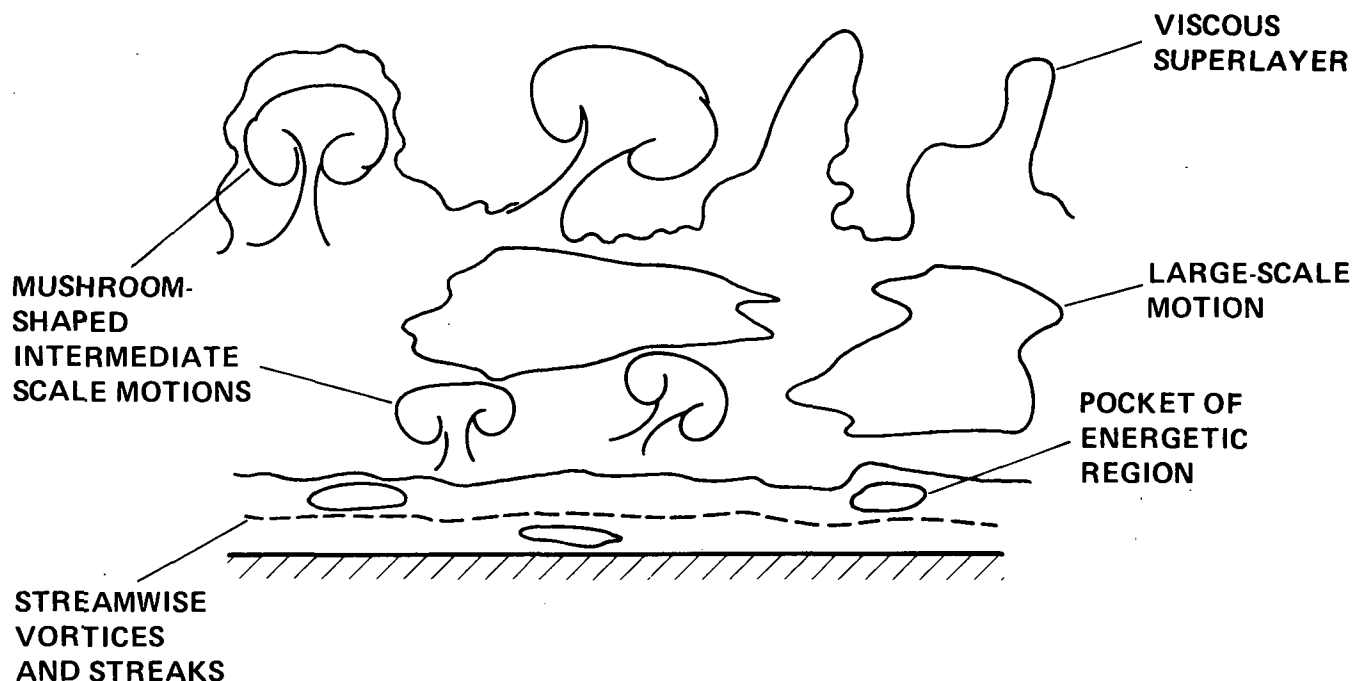


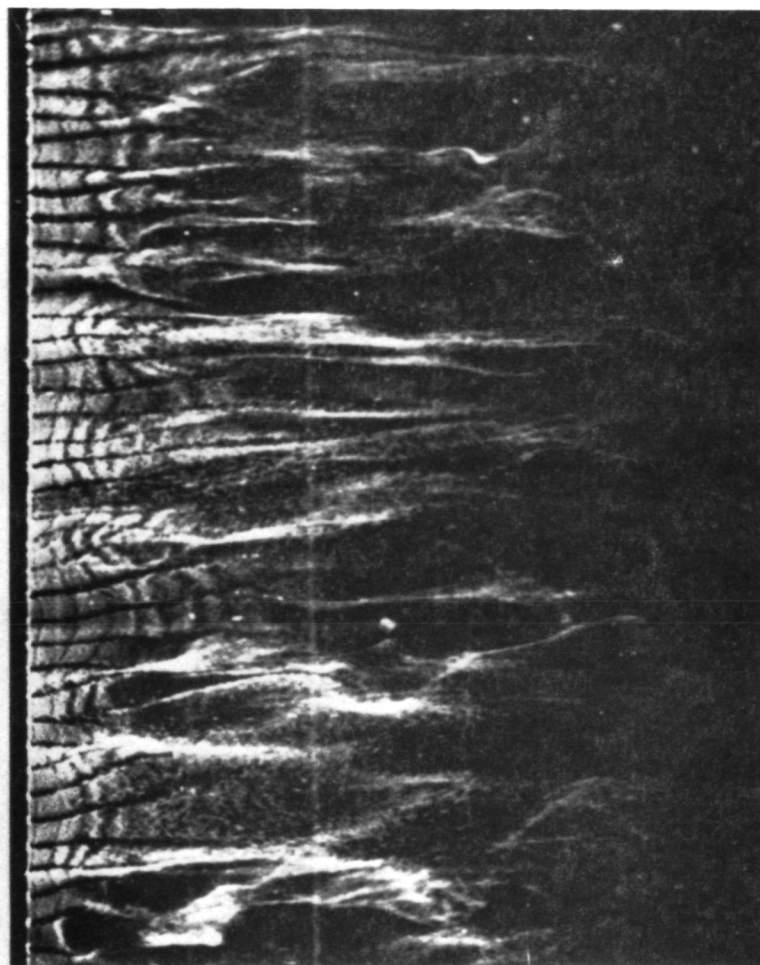
Figure 12. - Schematic of organized structures in the turbulent boundary layer.

called an ejection, are primary sources of the continual production of turbulence in the wall layer. Observations of the length of these structures vary from $x^+ = 100$ to $x^+ = 2000$ (refs. 110-112); the vertical extent varies from $y^+ = 20$ to $y^+ = 50$, and the mean spanwise extent between vortex centers is 50 wall units, with a possible dependence on Reynolds number (ref. 113). The streamwise streaks interact with the outer flow when they break up, following lift-up and oscillation, during a "bursting" (ref. 114) process. For the last 10 years, the mean dimensionless time between bursts was considered to be determined by the outer scaling variables, $U_\infty T / \delta \approx 6$ (ref. 115). Recently, it has been shown that the inner variables are considered to be the appropriate scaling variables (refs. 104, 116).

The bursting process leaves a pocket of energetic, intermediate-scale motions in a region $y^+ \approx 5$ and 40. Pockets lead to the formation of streamwise vortices and hairpin vortices. The period of formation of pockets is $u_\tau^2 T / \nu \approx 25$, and their dimensions are not easy to identify. Cantwell (ref. 105) estimates the streamwise length of an energetic pocket to range from 20 to 40 wall units and its normal extent to vary from 15 to 20 wall units. However, Falco (ref. 104) reports streamwise scales between 50 and 90 wall units. There is no direct information about the spanwise extent. These energetic pockets persist over a distance between 0.5δ and 1.5δ and travel at about $(0.65 \pm 0.05)U_\infty$. Instantaneous maximum Reynolds shear stress is very large compared with the local mean value during bursting; for example, at $y^+ \approx 30$, it can exceed 60 times the local mean value (ref. 117).

In the outer layer, flow is fully turbulent, but intermittent for $y > 0.4\delta$. Two different structures have been observed in this layer. One occurs in its interior and the other at its inner and outer edges. In the interior relatively large-scale energetic

MEAN
FLOW
DIRECTION



$$y^+ = 6.6$$

EXPERIMENT

Figure 13. - Structure of turbulent boundary layer visualized by passive markers introduced along a horizontal wire (courtesy of S. J. Kline).

motions are observed. At a height of about 0.8δ , the streamwise and spanwise extent of the large-scale motions varies between δ and 2δ , and between 0.5δ and δ , respectively. Further, the centers of these motions are spaced about 2 to 3 times δ in the spanwise direction. The distance over which they persist is about 1.8δ , and they travel with a speed of about $0.85U_\infty$. Instantaneous maximum shear stress owing to fluctuating velocities may exceed 10 times the local mean value.

Along the edges of the outer flow, mushroom-shaped, intermediate-scale, energetic regions are observed. These are called "typical eddies" by Falco (ref. 118). They have the streamwise and normal length, respectively, of about 200 and of $O(100)$ wall units between $730 \leq Re_\theta \leq 3.9 \times 10^4$ (ref. 118). The scales of typical eddies are Reynolds-number dependent. At very low Reynolds numbers, they are $O(\delta)$, and they appear to be the large-scale motions. These regions exist approximately over a distance 5 times their own streamwise extent and they also travel at about $0.85U_\infty$. The energetic motions that are just above the wall layer, interact with wall layer leading to the

formation of energetic pockets. Lifted fluid filaments in the wall layer may evolve into a mushroom-shaped energetic regions moving into the outer region. These regions scale with the Taylor microscale and they account for a major part of the Reynolds stresses (ref. 118).

The outer layer is bounded by the laminar-like viscous superlayer, outside of which vorticity fluctuations are zero, but velocity fluctuations are not. The superlayer is of the order of Kolmogorov length scale, η . The propagation velocity of the superlayer normal to itself is proportional to the Kolmogorov velocity scale, $v_\epsilon \equiv (\nu\epsilon)^{1/4}$ (refs. 99, 108).

From the above description of three-dimensional, unsteady turbulent boundary layer, it is concluded that the wall layer and the outer energetic regions are important. These regions need appropriate treatment in any direct or large-eddy simulation. As a turbulent boundary layer is an elliptic region, the wall layer and the outer layer interact, and the cause and effect cannot be separated.

Structure of the Mean Turbulent Boundary Layer

For a laminar velocity profile, we can use the concept of Reynolds similarity, but such a concept does not hold for a turbulent mean-velocity profile. These two velocity profiles greatly differ in both external and internal flows. The time-averaged turbulent velocity profile is made of two layers, an inner layer and an outer or core layer (fig. 14). The inner layer is adjacent to the wall and is divided into two layers, the viscous sublayer and the log-law region or the inertial sublayer. Further, the viscous sublayer is composed of the linear sublayer and the buffer layer. The outer layer is also subdivided into two regions. Proceeding away from the wall these are the wake-law layer and the viscous superlayer. The velocity and length scales, based on measurements and dimensional analysis, are identified below for a constant-density, two-dimensional mean flow over an impermeable smooth wall.

The inner layer of a wall shear layer extends about 10% — 20% of the boundary-layer thickness. The characteristic velocity scale and length scale are, respectively, u_τ and (ν/u_τ) , where u_τ is the friction velocity. These are known as the inner scales. The thicknesses of the linear sublayer, the buffer layer, and the log-law region are, respectively, $0 < y^+ \leq 5$, $5 \leq y^+ \approx 40$, and from $y^+ \approx 40$ to 500 — 1000 wall units. These bounds are, of course, approximate. Actually, the logarithmic law of the wall can be used from $y^+ = 30$, but the eddy viscosity assumes a linear variation with y^+ only above $y^+ \approx 50$ when the direct effect of viscosity is negligible (ref. 119). The thickness of the inner layer is about 0.1δ ($y^+ \approx 500$) at the lowest Reynolds number at which turbulent flow can be maintained, that is, at $Re_\theta \approx 320$, where Re_θ is a momentum-thickness Reynolds number (ref. 120). The linear sublayer is of the order of 0.001 to 0.01δ , depending on the Reynolds number.

In the linear sublayer, the Reynolds stresses are negligible, the pressure gradient has little effect, and the averaged velocity varies linearly. In the buffer layer, both viscous and Reynolds shear stresses are of the same order of magnitude, and there is

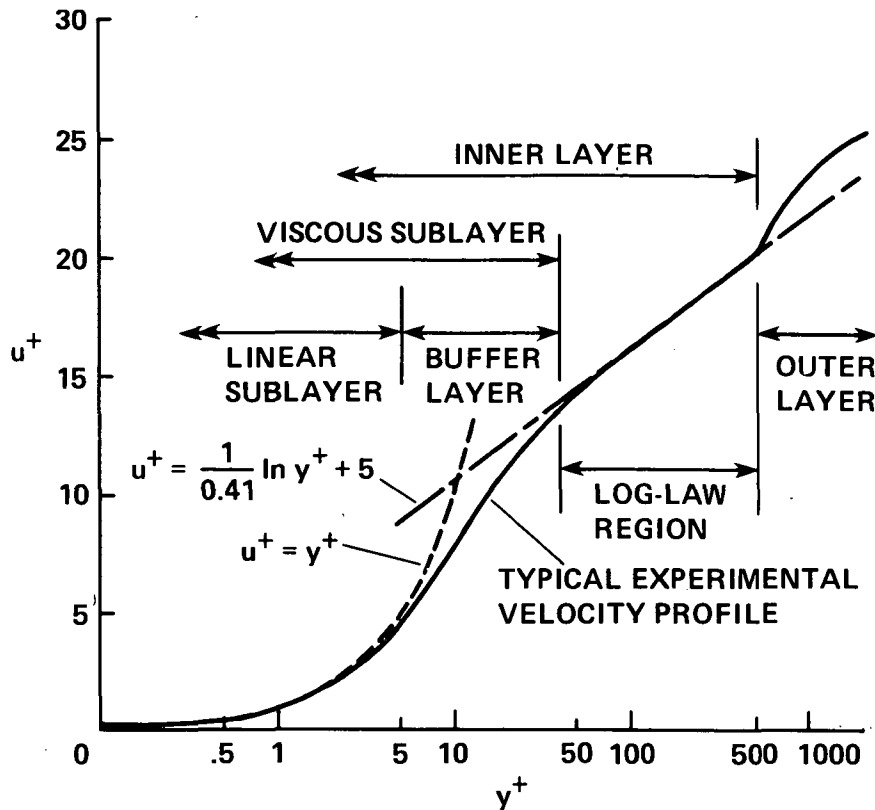


Figure 14. - Mean turbulent velocity in wall-layer nomenclature.

no simple variation of velocity with the normal distance. In the log-law region, the viscous stresses are negligible compared with the Reynolds stresses. Both the buffer and inertial layer are affected by the streamwise pressure gradient. At the end of this region, the mean velocity is about 70% of the velocity at the edge of outer layer in small-pressure-gradient flows.

The outer layer of an external shear layer contains 80% — 90% of the boundary-layer thickness. In the wake-law region, the characteristic velocity scales and length scale are, respectively, u_τ and U_∞ and δ for zero pressure gradient flows. This region is bounded by the viscous superlayer. The laminar-like superlayer is likely to be at least as thick as the turbulent viscous sublayer. In fully developed internal flows there is no superlayer. With decreasing Reynolds number, both viscous sublayer and superlayer become thick, and the wake region ultimately disappears at $Re_\theta \approx 500$ (ref. 122). Further, the mixing length and the dissipation-length parameter increase as Reynolds number decreases; see for example, reference 123. The ratio of the viscous superlayer length-scale to δ becomes independent of Reynolds number above $Re_\theta \approx 5000$ (ref. 123).

The above scales are valid, for both internal and external flows, provided the total shear stress varies slowly or is nearly constant in the normal direction. These scales are affected by surface nonuniformities and by the surface pressure gradient, if the latter is not small relative to the normal shear stress gradient at the wall, $\partial \tau_w / \partial y$.

In a computation, it is possible to use a "law of the wall" as a boundary condition instead of resolving the viscous sublayer. However, one of the tentative conclusions of the 1980-81 AFOSR-HTTM-Stanford Conference on Complex Turbulent Flows was that it is somewhat better to integrate the governing equations representing a turbulent boundary layer all the way to the wall than to assume a law of the wall (ref. 121). The evaluation committee, therefore, recommended an integration to the wall, except in special cases.

Thin- and Slender-Shear Layers

With s as the streamwise coordinate, a shear layer, whose thickness is δ at a distance L from its origin, is considered to be thin if $\partial\delta/\partial s$ is of order δ/L and is much smaller than unity, that is $\partial\delta/\partial s \ll 1$ (fig. 9). Note that it is the local rate of change that matters. In this case, the Navier-Stokes equations reduce to the thin-shear-layer equations. These latter equations are useful only if they are in a coordinate system such that s is in the direction of the thin-shear-layer. When this thin-shear-layer approximation is applicable, the ratio of neglected to retained stress gradients is $O[(\partial\delta/\partial s)^2]$ for laminar flows and $O(\partial\delta/\partial s)$ for turbulent flows (see, for example, ref. 65). Since, $(\partial\delta/\partial s)$ is generally larger in turbulent flows than in laminar flows, this approximation is less accurate in turbulent flows. Typically, the neglected streamwise viscous diffusion and turbulent diffusion are, respectively, $O(5.3Re^{-1})$ and $O(0.37Re^{-1/5})$ for $Re \leq 10^7$.

A shear layer is considered to be slender, if it is thin in two directions normal to the streamwise direction. In slender-shear-layers, the Reynolds shear-stress gradients dominate the streamwise momentum equation and the Reynolds normal-stress gradients affect any secondary flow.⁴ Only the streamwise gradients of viscous and Reynolds stresses can be neglected in the governing equations. This approximation gives the slender-shear-layer equations (ref. 124).

Triple-Deck Region

In laminar flows, the triple-deck theory (ref. 74) is applicable in the vicinity of separation point on a smooth surface, at the trailing edge of a flat plate, and in the neighborhood of a weak shock wave interacting with a boundary layer. This asymptotic theory is valid over a short distance. It gives the extent of this distance to be $O(Re^{-3/8}L)$ in the streamwise direction (fig. 15). Here Re , the Reynolds number, is based on L and local inviscid conditions, and L is a representative length of the boundary layer. The lateral scales of the lower, main and upper decks are, respectively, $O(Re^{-5/8}L)$, $O([Re^{-1/2} - Re^{-5/8}]L)$, and $O([Re^{-3/8} - Re^{-1/2}]L)$. Note that $O(Re^{-1/2}L)$ is the boundary-layer thickness. The upstream influence of the streamwise viscous stress gradient is felt only over a region of $O(Re^{-3/4}L)$ within the

⁴The motion in the plane perpendicular to the streamwise direction is called the secondary flow. In general, the streamwise component of vorticity is nonzero in secondary flows.

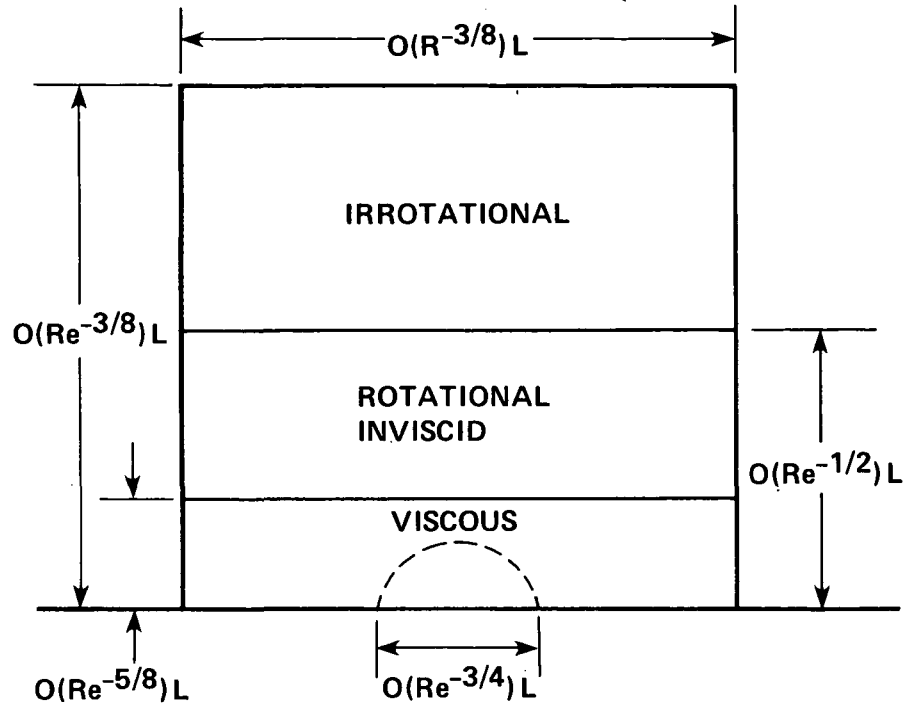


Figure 15. - Dimensions of the triple-deck region (based on ref. 74).

lower deck and centered, for example, on the trailing edge of the flat plate. On the other hand, the upstream influence of the pressure field is noticed over the length of this deck. It would be prudent to resolve the above asymptotic length scales in numerical computations of problems that are amenable to the triple-deck theory. Burggraf et al. (ref. 125) demonstrated this requirement on grid-spacing.

In the above examples, the contribution of the streamwise viscous gradient in the lower deck is relatively negligible; therefore, the thin-shear-layer approximation is valid, and the composite thin-shear-layer equations are applicable to small separated regions. In catastrophic or large separation regions, in which the flow is not laminar everywhere at moderate or high Reynolds numbers, the relative upstream influence of streamwise stress gradients needs to be quantified.

Shock-Wave/Turbulent-Boundary-Layer Interaction Region and Trailing Edge of a Flat Plate in a Turbulent Flow

When the turbulent boundary layer remains unseparated, the asymptotic length scales for shock-wave/boundary-layer interactions and trailing-edge flows have been reviewed by Melnik (ref. 66). The overall structure of the former case with a weak shock wave is similar to that of the latter case. In case of a weak normal shock-wave/boundary-layer interaction, the streamwise length of interaction is $O(\kappa^{3/2})$ where $\kappa \equiv (\ln Re)^{-1} \approx 0.05$ (typically) normalized by L (fig. 16). The lateral dimension of the lower deck, blending deck, main deck, and outer deck are, respectively, $O(\kappa \hat{\kappa})$,

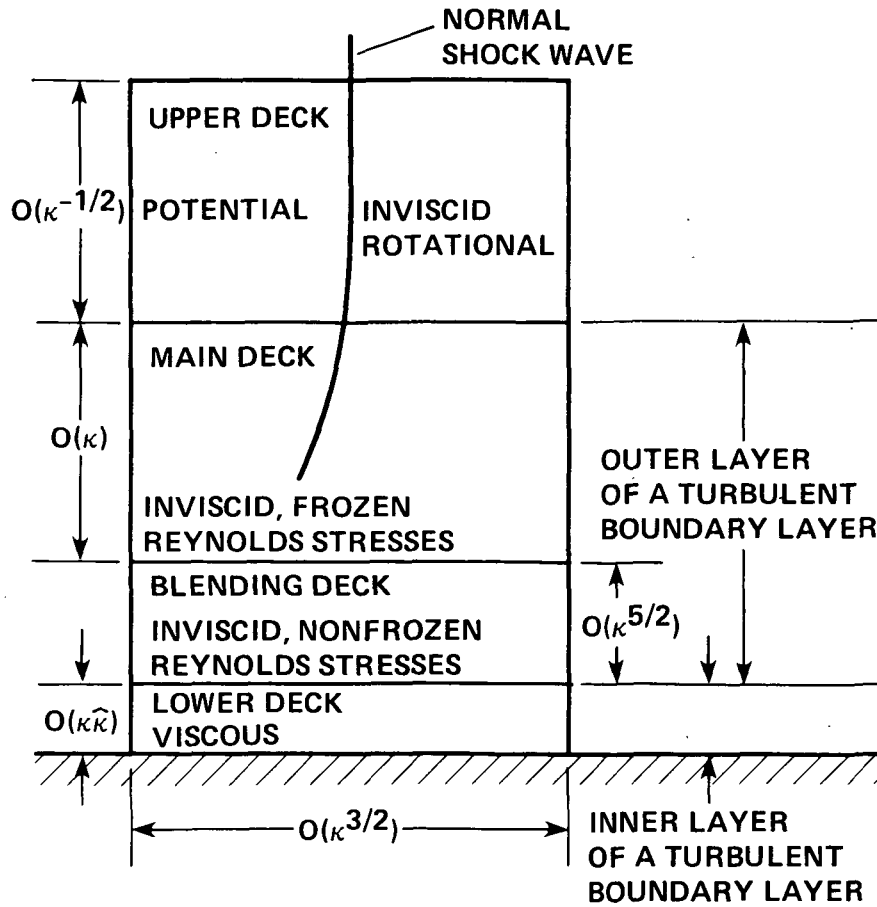


Figure 16. - Four-deck region for a weak normal shock wave interacting with a turbulent boundary layer (based on ref. 66).

$O(\kappa^{5/2})$, $O(\kappa)$, and $O(\kappa^{-1/2})$, where $\hat{\kappa} \equiv (\kappa^2 Re)^{-1}$. In case of a turbulent flow past a trailing edge of a flat plate or a cusped trailing edge of an airfoil, the streamwise length of interaction is $O(\kappa)$ (fig. 17). The lateral dimension of the lower deck, blending deck, main deck, and outer deck are, respectively, $O(\kappa\hat{\kappa})$, $O(\kappa^2)$, $O(\kappa)$, and $O(\kappa^{-1/2})$. In addition, there is an inner wall layer within the wall layer, whose streamwise length is $O(\kappa\hat{\kappa})$ and the lateral width is the same as that of the wall layer. In this region, the Navier-Stokes equations are required.

The nonasymptotic length scales for shock-wave/boundary-layer interactions are discussed by Inger (refs. 78, 126, 127).

Classification of Viscous-Inviscid Interactions

The nature of a viscous-inviscid interaction is identified by the thickness of the shear layer or the displacement thickness. When a shear layer suddenly thickens, the interaction is classified as a strong viscous-inviscid interaction. For example, on a smooth surface and in negligible pressure gradient, if the boundary-layer thickness is almost either

$$\delta = 5.3Re^{-1/2}L \quad (1)$$

for laminar flow or

$$\begin{aligned} \delta &= 0.37Re^{-1/5}L, & 5 \times 10^5 \leq Re \leq 10^7 \\ \delta &= \left(\frac{0.0598}{\log_{10}Re - 3.170} \right)L, & Re > 10^7 \end{aligned} \quad (2)$$

for turbulent flow (ref. 128), before, during, and after the viscous-inviscid interaction, then it is considered to be weak. When a shear layer sharply thickens and subsequently becomes larger than this magnitude, the interaction is considered to be a strong interaction.

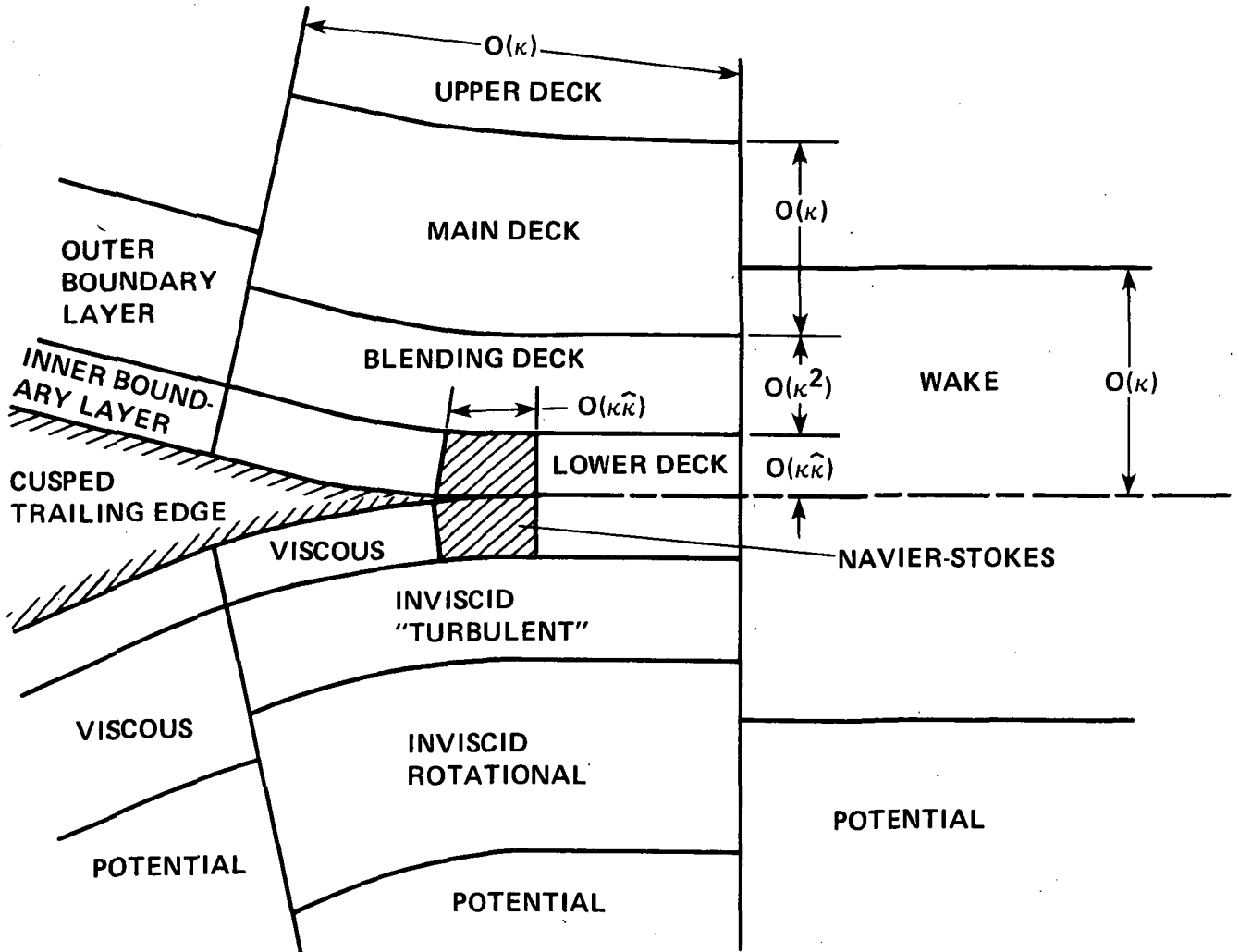


Figure 17. - Asymptotic flow-field structure around a cusped trailing edge of an airfoil in a turbulent flow (based on ref. 66).

Thickness of Shock Waves

The effect of viscosity and heat conductivity develops a continuous change of flow variables through a shock wave, which is an internal transitional or "boundary" layer. The shock wave is quite thin outside any viscous region. The thickness of the wave increases when the wave begins to interact with the viscous boundary layer, giving rise to a shock layer. This layer may even lose its identity as it penetrates into the viscous region. A turbulent boundary layer thickens the shock wave more than a laminar boundary layer.

At a Mach number of 1.05 and a Reynolds number of 10^7 with $L = 1$, the shock thickness in air is almost the same as the thickness of the linear sublayer of a turbulent boundary layer on a smooth flat surface. Another estimate is given by Taylor and Maccoll (ref. 129) for a weak shock wave, in which the total speed change is small compared with the speed of sound. They give the thickness of the region within which eight tenths of the change from U_1 to U_2 occurs as $T = 1/(U_1 - U_2)$ cm for air. When the change in velocity through a shock wave is one tenth the speed of sound, that is, 30 m/sec, the shock thickness is 3×10^{-4} cm, which is comparable to the thickness of the linear sublayer at the above Reynolds number. (Lagerstrom, ref. 130, also states that the thickness of the shock wave is of the order of 2μ for air.) From measurements of shock wave structure, Sherman (ref. 131) found that the Navier-Stokes equations are valid within the shock wave up to a Mach number of 2. This conclusion is considered to be somewhat cautious by Lagerstrom (ref. 130).

Scales of Strain Rates

Frequently, turbulence in thin-shear-layers is modeled by eddy-viscosity formulas such that turbulent shear stress is proportional to averaged rate of shear strain, $\partial u_s / \partial n$, where u_s is the velocity in the streamwise direction s and the normal direction is represented by n . This model satisfactorily predicts only simple shear layers in which any extra strain rate, e , does not affect the turbulence structure. When $e/(\partial u_s / \partial n) < 0.001$ (approximately), Bradshaw (ref. 65) considers any additional strain rate unimportant. In complex shear layers, the extra strain rates affect the turbulence structure. Although the thin-shear-layer approximation is valid when $e/(\partial u_s / \partial n) < 0.01$, the above eddy-viscosity model must be modified. If $0.01 < e/(\partial u_s / \partial n) < 0.1$, the thin-shear-layer approximation is also not valid and some of neglected terms of the Navier-Stokes equations are approximated in the governing equations. When $e/(\partial u_s / \partial n) > 0.1$, we have what Bradshaw classifies as strongly distorted flows.

Temporal Scales

Temporal scales are determined by the frequency of an unsteadiness, which may be either externally induced or self-induced. Externally induced unsteadiness may be due to fluctuations of boundaries or of the free stream or to initial conditions. Self-induced unsteadiness is developed by hydrodynamic instability, for instance, transitional flows, turbulent flows, and vortex shedding from bluff bodies. Typically laminar flow problems

may involve externally imposed unsteadiness, whereas turbulent flow problems may contain externally or self-induced unsteadiness or both. There may be a coupling between externally induced and self-induced unsteadiness. For example, unsteady forces and moments owing to vortex shedding from a bluff body may force the body to move, if it is not perfectly rigid, which in turn may change the shedding frequency. Unsteadiness can be completely stochastic, highly organized, or a combination of random and periodic components which under certain conditions may interact with each other. Further, there may be a single narrow-band frequency or a broad band of frequencies. Transitional and turbulent flows are characterized by a wide range of frequencies as discussed above. But the externally induced unsteadiness is usually driven by a discrete frequency, which determines the dominant temporal scale. From a computational point of view, the highest significant frequency must be resolved. This fixes the computational time-step.

When a flow field is oscillating with a dominant frequency, f , the Strouhal number, $St = fL/U_\infty$, is used for identifying the time-scale of importance. This number characterizes the relative importance of the local velocity (acceleration) with respect to the convective velocity (acceleration), that is, the time-scale of physical motion to the basic fluid dynamic time-scale. For slender-body oscillations, the reduced frequency, $k = \omega L/U_\infty$, is the relevant nondimensional parameter where $f = \omega/2\pi$. If St is referred to the speed of sound instead of U_∞ , a necessary condition for the fluid to behave as if it were incompressible is that $St^2 \ll 1$.

When the imposed unsteadiness is gradual so that the viscous diffusion is able to keep pace with the change, there is a quasi-steady flow. But if changes are rapid relative to the diffusion process, the unsteadiness is confined to a layer, called the Stokes layer, thinner than the boundary layer. Obviously, the flow cannot then be treated as quasi-steady. The diffusive time-scale is $O(\delta^2/\nu)$ for diffusion of vorticity and momentum outward from the body surface. For a body moving from rest, the boundary-layer thickness is $O[(\nu t)^{1/2}]$ at small times. For an oscillatory body, the boundary-layer thickness is $O[(\nu/\omega)^{1/2}]$.

When the flow variables are decomposed into a mean field and a fluctuating field, and with the fluctuating velocity components that satisfy the Reynolds conditions (ref. 132) as constraints, the time-averaged equations of motion are appropriate for computation of unsteady flows, provided the averaging time-interval is large compared with the periods characteristic of time-scales that cannot be resolved computationally, but small compared with the period of mean unsteady motion. This double decomposition of the velocity field is satisfactory for many physical problems involving relatively small-amplitude and small-frequency oscillations. The above decomposition has limitations, however, as any harmonics higher than the first may become indistinguishable from the random fluctuations caused by turbulence. Further, the mean effects of small scales on large scales and vice versa are not discernible. Broad ranges of scales, therefore, require at least a triple decomposition of the velocity field with three different velocity, length, and time scales.

When the turbulence structure is unaffected by externally induced unsteadiness, steady-flow turbulence models can be used to predict unsteady turbulent flows. Above a

critical frequency, the turbulence structure is affected by externally imposed unsteadiness and steady-flow models cannot be used. In zero pressure gradient flows, the value of this critical frequency ranges from 20% to 100% of $f_b = U_\infty/(5\delta)$, which is roughly the burst frequency based on outer scales (refs. 133-136). In adverse pressure gradient flows, the critical frequency is well below this burst frequency. Values of 6% to 28% of f_b have been reported (refs. 137-139).

Additional discussion concerning temporal scales is presented by Cousteix et al. (ref. 140), Carr (ref. 141) and Chapman (ref. 142).

SIGNIFICANCE AND GENERATION OF VORTICITY

The concept of a vortex has been used since prehistoric times to describe natural phenomena (ref. 143). In historic times, the analysis of vortices was applied to explain such phenomena as the evolution of the universe, the motions of celestial bodies, and atomic structure of matter. These efforts were unsuccessful and ended. But with the development and application of Helmholtz's vortex theory (ref. 144) within the realm of classical mechanics, this concept has had an enormous effect on fluid dynamics.

Significance of Vorticity

A mathematical term used by Euler and d'Alembert, which later was identified as vorticity (ref. 145), has had a profound effect on the study of fluid motions. In an inviscid fluid a vortex is defined as a finite volume or area of rotational fluid, bounded by irrotational fluid or solid walls (ref. 146). Viscosity smooths out discontinuities or singularities. Therefore, in a viscous fluid, a vortex is identified by closed equivorticity lines with a relative extremum of vorticity inside the innermost closed loop (refs. 147, 148), as seen in figure 18. This identification depends on rotation of the reference frame and on stratification (refs. 149, 150). Therefore, Lugt (ref. 149) has defined a vortex as the rotating motion of a multitude of material particles around a common center.

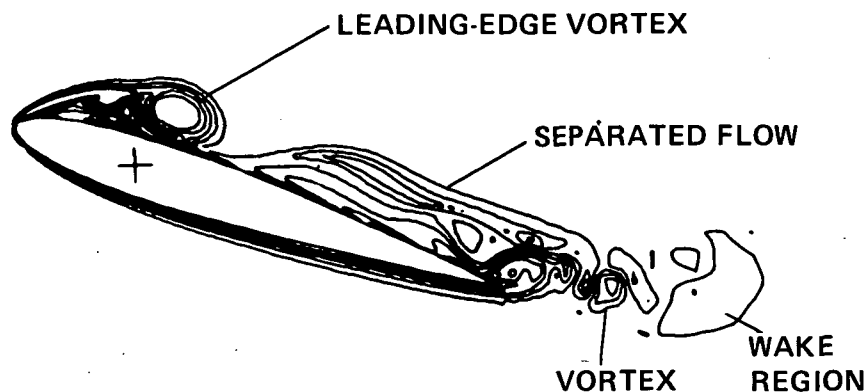


Figure 18. - Equivorticity lines around an oscillating airfoil (ref. 148).

Vortices and vortex motions are "the sinews and muscles of fluid motions" (ref. 151). They are omnipresent in separated flows and in many types of turbulent flows; see for instance references 146, 149, and 152. In many cases, vortices are formed by an ejection, at a salient edge or from a smooth surface, of the vortical boundary-layer fluid into the main body of fluid where viscosity plays a negligible role. In some cases, they are formed next to a boundary by shear in the external flow. Turbulent flow structures, organized or not organized, are essentially vortices. For example, a mixing layer consists of a row of quasi-two-dimensional organized structures (refs. 146, 153). Also such structures may be found in jets, wakes, and boundary layers. Organized vortices are ordered structures of fluid motion.

Some vortex patterns and interactions may be represented by a combination of the inviscid and viscous models, by suitably dividing the flow domain, and some may be represented by only viscous-flow models. When circulation cannot be convected out of a closed separated region (a separation bubble), viscosity plays an important role along with convection and possibly vortex stretching.

The significance of the vorticity vector, which is defined as the curl of the velocity vector, is really mathematical rather than physical. This significance is specifically for the understanding and mathematical description of the study of fluid flow of a uniform, incompressible fluid or a homentropic fluid (that is, uniform entropy per unit mass over the fluid), when the direct effect of viscosity may be neglected. In general, the nature and structure of the laminar or turbulent flow are controlled by the vorticity field. Vorticity considerations illuminate the detailed development of any rotational flow just as clearly as do momentum considerations, and allow a compact description of the kinematics and dynamics of fluid motions. At high Reynolds numbers, the vorticity field is confined to thin layers or fine tubes, whereas the velocity vector is present in the whole flow field. In addition, study of this field is the most enlightening in understanding how the nonlinearity of the equation of motion generates highly complicated solutions that represent turbulent flows.

Generation of Vorticity

Although one cannot see the vorticity field and although its measurement is difficult, its presence in aerodynamic applications is easily detected by the determination of circulation, Γ , which is defined as the line integral of the velocity field around any closed curve. Kelvin's theorem of circulation (ref. 154)

$$\frac{D\Gamma}{Dt} = \oint \left(-\frac{\nabla p}{\rho} \right) \cdot d\underline{\ell} + \oint \frac{1}{\rho} (-\nabla \times [\mu \underline{\Omega}] + \nabla[(4/3)\mu \nabla \cdot \underline{U}]) \cdot d\underline{\ell} + \oint \underline{\mathcal{F}} \cdot d\underline{\ell} \quad (3)$$

shows that the time rate of change of circulation associated with a closed curve l , always made up of the same fluid particles, is governed by the torques produced as a result of pressure forces, viscous forces, and body forces. In the above equation, ρ , p , $\underline{\Omega}$, μ , \underline{U} , and $\underline{\mathcal{F}}$ are, respectively, density; pressure; the vorticity vector; the dynamic viscosity, with the second coefficient of viscosity as $-(2/3)\mu$; the velocity vector; and the body force. The underline denotes a vector field. Irrotational body forces (i. e., conservative forces with single-valued force potential) do not produce circulation. Since

fluid dynamic problems, in general, contain such forces we have omitted the effects of the body force term in the following discussion.

If isobars and isochors in a fluid particle are parallel, the situation is described as barotropic. In this case, the density field is function of the pressure field alone, the pressure forces do not produce circulation. In an inviscid incompressible fluid of uniform density and in an inviscid compressible fluid, provided the flow field is homentropic, there are no internal sources of vorticity. On the other hand, in a compressible, nonhomentropic fluid, pressure forces provide internal sources of vorticity. When all the torque-producing agents are absent, the dynamics of the fluid is governed by Helmholtz's vortex laws (ref. 144).

If the sources of vorticity owing to pressure are absent, vorticity flux or circulation cannot be created in the interior of the fluid; see references 155 and 156. In such cases it is generated by viscous forces at a solid boundary or at a free surface.

According to Vazsonyi (ref. 157), Hadamard (ref. 158) was first to point out that vortices are generated by shock waves and that the flow is no longer barotropic after shock waves. This is demonstrated by the Crocco-Vazsonyi equation (ref. 157) for steady flow of an inviscid fluid

$$\nabla H = T \nabla S + \underline{U} \times \underline{\Omega} \quad (4)$$

where H , T , and S are, respectively, total enthalpy, temperature, and entropy. The vorticity vector, therefore, depends on the rates of change of entropy and enthalpy normal to streamlines. When all streamlines have the same H but different entropy, there is production of vorticity. This is the situation downstream of a curved shock wave, because the entropy increase across a shock wave is determined by the local angle of the shock. Even if the flow upstream a shock wave were to be irrotational, the flow downstream of a curved shock wave is rotational.

The vorticity field in a Newtonian fluid is governed by the vorticity equation,

$$\frac{D\underline{\Omega}}{Dt} = (\underline{\Omega} \cdot \nabla) \underline{U} + \nabla \times \left(-\frac{\nabla p}{\rho} \right) + \nabla \times \left[\frac{1}{\rho} (-\nabla \times (\mu \underline{\Omega}) + \nabla [(4/3)\mu \nabla \cdot \underline{U}]) \right] \quad (5)$$

which is obtained by taking the curl of both sides of the equation of motion. This equation shows that the time rate of change of vorticity as one follows the fluid is produced by a nonlinear, inviscid extension or contraction and tilting of existing vorticity by the strain rate, a source of vorticity resulting from the pressure force and diffusion of vorticity by viscosity. Tilting of a vortex line or tube changes the relative magnitude of vorticity components and its stretching concentrates the vorticity in a smaller volume. When a flow is two-dimensional, the vorticity stretching and tilting term is absent; and when the fluid is incompressible, the source term is absent.

Production of circulation generally means generation of vorticity, as circulation is a measure of integrated vorticity field; but a change in vorticity does not necessarily change circulation. This is readily noticed by comparing equations (3) (without the body force term) and (5). Both have pressure and viscous terms, but the term $(\underline{\Omega} \cdot \nabla) \underline{U}$ in equation (5) has no counter part in equation (3). The vorticity of a material element

increases when it is extended in the direction of the local vortex line. If the above torque-producing elements are absent, the circulation is the same for every contour enclosing the vortex line, the ratio of vorticity to the product of density and the length of the line remains constant, and vortex lines remain located to the same elements of the fluid forever. But for the action of viscosity, the intensification of vorticity by extension of vortex lines continues. The total amount of vorticity in a body of fluid increases, until through change of the vorticity field the smoothing effect of viscosity is able to balance or exceed this gain. This is one of the most remarkable characteristics of turbulent flows.

When a solid body is passed through a viscous fluid that is void of vorticity, vorticity is imparted to the fluid through the mechanism of the viscosity and it is diffused into the interior of the fluid again by the action of viscosity. The no-slip boundary condition applied to the Navier-Stokes equations gives the instantaneous local rate of generation of positive and negative vorticity per unit area, per unit time, in terms of the strength of the vorticity source given by $(\nabla p)/\rho$. The pressure gradient along the surface of the body creates vorticity tangential to the surface. The maximum value of absolute vorticity need not be at the surface, but it could be in the interior of the fluid near the surface. This mechanism of vorticity generation is altogether absent in free shear layers. In case of a free surface, a nonzero jump in velocity derivative is responsible for generation of vorticity (ref. 156).

The mean level of vorticity in a turbulent flow is also changed because of the production of vorticity by the Reynolds stresses arising from fluctuating velocity and vorticity fields. This is shown for an incompressible fluid. Instantaneous values \underline{U} and $\underline{\Omega}$ are decomposed into the mean and fluctuating values. This is expressed by the relation

$$f = \bar{f} + f' \quad (6)$$

where the over bar designates a mean or averaged value, and the prime denotes the remaining fluctuating value. After substituting such relations into equation (5), taking a short-time average of all terms in the equation constrained with the Reynolds conditions (ref. 132), multiplying by $\bar{\Omega}_i$, and rearranging terms, we obtain

$$\frac{D}{Dt} \left(\frac{\bar{\Omega}_i \bar{\Omega}_i}{2} \right) = \bar{\Omega}_i \bar{\Omega}_j S_{ij} - \bar{\Omega}_i \epsilon_{ijk} \frac{\partial^2 (\overline{u'_i u'_k})}{\partial x_j \partial x_l} + \nu \frac{\partial^2 \bar{\Omega}_i}{\partial x_j \partial x_j} \quad (7)$$

where S_{ij} , ϵ_{ijk} , u'_i , and ν are, respectively, the mean strain rate, the alternating tensor, fluctuating velocity, and the kinematic viscosity; the Cartesian tensor summation convention is used. The first term on the right-hand side is the stretching or contracting and tilting term, the second contains amplification or attenuation within averaging time of mean square vorticity caused by the stretching of fluctuating vorticity through fluctuating strain rates (see for example, ref. 159), and the last term represents viscous transport and dissipation of $\bar{\Omega}_i \bar{\Omega}_i$.

It is a fundamental property of turbulent flows that nearby points tend to move apart because of the diffusive action of turbulence. As a result, on the average, vortex lines and vortex sheets tend to be stretched rather than contracted. Therefore, the above stretching terms represent a growth of vorticity, limited only by viscous

dissipation. The continued process of vortex stretching implies a cascade of energy from large-scale vortex motions to small-scale motions resulting in larger and larger velocity gradients.

REFERENCES

1. Lomax, H.; and Mehta, U.: Some Physical and Numerical Aspects of Computing the Effects of Viscosity on Fluid Flow, *Viscous Flow Computational Methods*, Vol. 3 in the Series on Recent Advances in Numerical Methods in Fluids, W. G. Habashi, ed., Pineridge Press Ltd., Swansea, U. K., 1984.
2. Euler, L.: *Principes Généraux du Mouvement des Fluides*, Hist. de l'Acad. de Berlin, 1755.
3. d'Alembert, J. le Rond: *Essai d'une Nouvelle Theorie de la Resistance des Fluides*, Paris, 1752.
4. Newton, I.: *Philosophiae Naturalis Principa Mathematica*, Book II, London, 1726.
5. Navier, C. M. L. H.: Mémoire sur les Lois du Mouvement des Fluides, *Mém. de l'Acad. des Sciences*, vol. 6, 1826, pp. 389-416.
6. Poisson, S. D.: Mémoire sur les Équations Générales de l'Équilibre et du Mouvement des Corps Solides Élastiques et des Fluides, *Journal de l'Ecole Polytechnique*, Paris, vol. 20, 1831.
7. Saint-Venant, B. de: Note à Joindre au Mémoire sur la Dynamique des Fluides, *Comptes Rendus Acad. Sci. Paris, Ser. A*, vol. 17, 1843, pp. 1240-1242.
8. Stokes, G. G.: On the Theories of Internal Friction of Fluids in Motion, *Trans. Cambridge Philos. Soc.*, vol. 8, pt. III, 1847, pp. 287-305.
9. Helmholtz, H. von: Über Discontinuirliche Flüssigkeitsbewegungen, *Monatsberichte der königl. Akademie der Wissenschaften*, Berlin, vol. 23, 1868, pp. 215-228. (Also *Phil. Mag.*, vol. 36, Nov. 1868, p. 337.)
10. Kirchhoff, G.: Zur Theorie freier Flüssigkeitsstrahlen, *Crelle J. Math.*, vol. 70, 1869, pp. 289-298.
11. Rayleigh, Lord (Strutt, J. W.): Notes on Hydrodynamics, *Phil. Mag.*, Dec. 1876.
12. Prandtl, L.: Über Flüssigkeiten bei sehr kleiner Reibung, *Verhandlung des drittes Internationalen Mathematiker-Kongresses*, Heidelberg, 1904; Teubner, Leipzig, 1905, pp. 484-491. (NACA TM-452, 1928.)
13. Tani, I.: History of Boundary-Layer Theory, *Annu. Rev. Fluid Mech.*, vol. 9, 1977, pp. 87-111.
14. Blasius, H.: Grenzschichten in Flüssigkeiten mit kleiner Reibung, Dissertation, Leipzig, 1907. (*Z. Math. Phys.*, vol. 56, 1908, pp. 1-37.)

15. Stüper, J.: Reduction of Lift of a Wing Due to Its Drag, *Zeitschrift für Flugtechnik und Motorluftschiffahrt*, vol. 24, no. 16, August 1933. (Also NACA TM-781, 1935.)
16. Van Dyke, M.: Higher-Order Boundary-Layer Theory, *Annu. Rev. Fluid Mech.*, vol. 1, 1965, pp. 265-292.
17. Stewartson, K.: D'Alembert's Paradox, *SIAM Review*, vol. 23, no. 3, July 1981, pp. 308-343.
18. Goldstein, S.: On Laminar Boundary Flow near a Point of Separation, *Quart. J. Mech. Appl. Math.*, vol. 1, 1948, pp. 43-69.
19. Lighthill, M. J.: On Boundary Layers and Upstream Influence: II. Supersonic Flow without Separation, *Proc. R. Soc. London Ser. A*, vol. 217, 1953, pp. 478-507.
20. Müller, E.-A.: Theoretische Untersuchungen über die Wechselwirkung zwischen einer einfallenden kleinen Störung und der Grenzschicht bei schnell strömenden Gasen, Dissertation, Universität Göttingen, 1953.
21. Lees, L.; and Reeves, B. L.: Supersonic Separated and Reattaching Laminar Flows: I. General Theory and Applications to Adiabatic Boundary Layer/Shock Wave Interactions, *AIAA J.*, vol. 2, 1964, pp. 1907-1920.
22. Catherall, D.; and Mangler, K. W.: The Integration of the Two-Dimensional Laminar Boundary-Layer Equations past the Point of Vanishing Skin Friction, *J. Fluid Mech.*, vol. 26, 1966, pp. 163-182.
23. Neiland, V. Y.: Towards a Theory of Separation of the Laminar Boundary Layer in a Supersonic Stream, *Izv. Akad. Nauk SSSR Mekh. Zhidk. Gaza*, vol. 4, 1969, pp. 33-35.
24. Stewartson, K.: On the Flow near the Trailing Edge of a Flat Plate II, *Mathematika*, vol. 16, 1969, pp. 106-121.
25. Stewartson, K.; and Williams, P. G.: Self-Induced Separation, *Proc. Roy. Soc. London, Ser. A*, vol. 312, 1969, pp. 181-206.
26. Messiter, A. F.: Boundary Layer Flow near the Trailing Edge of a Flat Plate, *SIAM J. Appl. Math.*, vol. 18, 1970, pp. 241-257.
27. Jones, B. M.: The Streamline Aeroplane, *J. R. Aeronaut. Soc.*, vol. 33, 1929, pp. 357-385.
28. Jones, W. P.: Trends in Unsteady Aerodynamics: 6th Lanchester Memorial Lecture, *J. R. Aeronaut. Soc.*, vol. 67, 1963, p. 137.
29. Farren, W. S.: Reaction on a Wing Whose Angle of Incidence is Changing Rapidly, Wind Tunnel Experiments with a Short-Period Recording Balance, Aeronautical Research Committee R&M 1648, 1935.
30. McCroskey, W. J.: Some Current Research in Unsteady Fluid Dynamics, *Trans. ASME J. Fluid Eng.*, vol. 99, no. 1, March 1977, pp. 8-38.

31. Finke, K.: Unsteady Shock Wave-Boundary Layer Interaction on Profiles in Transonic Flow, *Flow Separation*, Paper no. 28, AGARD-CP-168, May 1975.
32. Meier, G. E. A.: Shock-Induced Flow Oscillations, *Flow Separation*, Paper no. 29, AGARD-CP-168, May 1975.
33. Garrick, I. E.: Aeroelasticity—Frontiers and Beyond, *J. of Aircraft*, vol. 13, no. 9, 1976, pp. 641-657.
34. Abramson, H. N.: Hydroelasticity: A Review of Hydrofoil Flutter, *Appl. Mech. Rev.*, vol. 22, no. 2, 1969, pp. 115-121.
35. Sisto, F.: A Review of the Fluid Mechanics of Aeroelasticity in Turbomachines, *Trans. ASME J. Fluids Engr.*, vol. 99, no. 1, 1977, pp. 40-44.
36. Kerrebrock, J. L.: Flow in Transonic Compressors, *AIAA J.*, vol. 19, no. 1, 1981, pp. 4-19.
37. *Unsteady Phenomena in Turbomachinery*, AGARD CP-177, Sept. 1975.
38. Platzer, M.: Unsteady Flows in Turbomachines—A Review of Current Developments, Paper no. 33, AGARD CP-227, 1977.
39. Lighthill, Sir M. J.: *Waves in Fluids*, Cambridge University Press, 1978.
40. Pearcey, H. H.: Hydrodynamics and Aerodynamics: Cross Fertilisation in Research and Design, *Aeronaut. J.*, January 1982, pp. 1-22.
41. Lighthill, Sir M. J.: *Mathematical Biofluidynamics*, SIAM, Philadelphia, Pa., 1975.
42. Birkhoff, G.: Numerical Fluid Dynamics, *SIAM Rev.*, vol. 25, no. 1, 1983, pp. 1-34.
43. Rogers, E. W. E.: Aerodynamics – Retrospect and Prospect, *Aeronaut. J.*, Feb. 1982, pp. 43-67.
44. Morkovin, M. V.: Instability, Transition to Turbulence and Predictability, AGARD-AG-236, 1978.
45. Reshotko, E.: Boundary-Layer Stability and Transition, *Annu. Rev. Fluid Mech.*, vol. 8, 1976, pp. 311-349.
46. Herbert, Th.; and Morkovin, M. V.: Dialogue on Bridging Some Gaps in Stability and Transition Research, Proceedings of the IUTAM Symposium on Laminar-Turbulent Transition, 1979, pp. 47-72.
47. Reynolds, O.: An Experimental Investigation of Circumstances Which Determine Whether the Motion of Water Shall be Direct or Sinuous, and of the Law of Resistance in Parallel Channels, *Philos. Trans. R. Soc. London*, vol. 174, 1883, pp. 935-982; *Scientific Papers*, Cambridge University Press, vol. 2, 1891, pp. 51-105.
48. Rayleigh, Lord (Strutt, J. W.): On the Question of the Stability of the Flow of Fluids, *Scientific Papers*, Cambridge University Press, vol. 3, 1892, pp. 575-584.

49. Reynolds, W. C.: Simulation of Turbulent Shear Flows: What Can We Do and What Have We Learned?, *Proceedings of the Seventh Biennial Symposium on Turbulence*, Rolla, Mo., Sept. 1981.
50. Townsend, A. A.: *The Structure of Turbulent Shear Flow*, First ed., Cambridge University Press, 1956.
51. Smagorinsky, J.: General Circulation Experiments with the Primitive Equations, 1, The Basic Experiment, *Mon. Weather Rev.*, vol. 91, 1963, pp. 99-164.
52. Lilly, D. K.: The Representation of Small-Scale Turbulence in Numerical Simulation Experiments, *Proceedings of the IBM Scientific Computing Symposium on Environmental Sciences*, 1967, pp. 195-210.
53. Deardorff, J. W.: A Three-Dimensional Numerical Investigation of the Idealized Planetary Boundary Layer, *Geophys. Fluid Dyn.*, vol. 1, 1970, pp. 377-410.
54. Deardorff, J. W.: A Numerical Study of Three-Dimensional Turbulent Channel Flow at Large Reynolds Number, *J. Fluid Mech.*, vol. 41, 1970, pp. 453-480.
55. Deardorff, J. W.: The Use of Subgrid Transport Equations in a Three-Dimensional Model of Atmospheric Turbulence, *Trans. ASME J. Fluids Eng.*, vol. 95, 1973, pp. 429-438.
56. Leonard, A.: On the Energy Cascade in Large-Eddy Simulations of Turbulent Fluid Flows, *Adv. Geophys.*, vol. 18A, 1974, pp. 379-385.
57. Clark, R. A.; Ferziger, J. H.; and Reynolds, W. C.: Evaluation of Subgrid-Scale Models Using an Accurately Simulated Turbulent Flow, *J. Fluid Mech.*, vol. 19, 1979, pp. 1-16.
58. Ferziger, J. H.; Mehta, U. B.; and Reynolds, W. C.: Large Eddy Simulation of Homogeneous Isotropic Turbulence, Presented at the Symposium on Turbulent Shear Flows, the Pennsylvania State U., University Park, Pa., Apr. 1977.
59. Moin, P.; Reynolds, W. C.; and Ferziger, J. H.: Large Eddy Simulation of Incompressible turbulent Channel Flow, Report TF-12, Department of Mechanical Engineering., Stanford U., Stanford, Calif., 1978.
60. Ferziger, J. H.: Higher-Level Simulations of Turbulent Flows, von Karman Institute for Fluid Dynamics, Computational Fluid Dynamics Lecture Series 1981-5, 1981.
61. Schumann, U.: Ein Verfahren zur Direkten Numerischen Simulation Turbulenter Strömungen in Platten- und Ringspaltkanälen und über seine Anwendung zur Untersuchung von Turbulenzmodellen, Ph. D. Thesis, Universität Karlsruhe, Karlsruhe, West Germany, 1973. (Also NASA TT F-15,391.)
62. Schumann, U.: Subgrid Scale Model for Finite Difference Simulations of Turbulent Flows in Plane Channels and Annuli, *J. Comp. Physics*, vol. 18, 1975, pp. 376-404.
63. Kim, J.; and Moin, P.: Large Eddy Simulation of Turbulent Channel Flow: ILLIAC IV Calculation, AGARD-CP-271, 1980.

64. Moin, P.; and Kim, J.: Numerical Investigation of Turbulent Channel Flow, *J. Fluid Mech.*, vol. 118, 1982, pp. 341-377.
65. Bradshaw, P.: Effects of Streamline Curvature on Turbulent Flow, AGARD-AG-169, Aug. 1973.
66. Melnik, R. E.: Turbulent Interactions on Airfoils at Transonic Speeds – Recent Developments, *Viscous-Inviscid Interactions*, AGARD-CP-291, 1980.
67. Adamson, T. C., Jr.; and Messiter, A. F.: Analysis of Two-Dimensional Interactions between Shock Waves and Boundary Layers, *Annu. Rev. Fluid Mech.*, vol. 12, 1980, pp. 103-138.
68. Williams, P. C.: A Reverse Flow Computation in the Theory of Self-Induced Separation, *Lecture Notes in Physics*, vol. 35, 1975, pp. 445-451.
69. Bradshaw, P.: Shear Layer Studies – Past, Present, Future, *Recent Contributions to Fluid Mechanics*, W. Haase, ed., Springer-Verlag, 1982.
70. Bradshaw, P.: Prediction of Separation Using Boundary Layer Theory, AGARD-LS-94, 1978.
71. Telionis, D. P.: *Unsteady Viscous Flows*, Springer Series in Computational Physics, Springer-Verlag, 1981.
72. Lock, R. C.; and Firmin, M. C. P.: Survey of Techniques for Estimating Viscous Effects in External Aerodynamics, Royal Aircraft Establishment, Technical Memorandum Aero 1900, 1981.
73. Le Balleur, J. C.: Strong Matching Method for Computing Transonic Viscous Flows Including Wakes and Separations – Lifting Airfoils, *La Recherche Aerospatiale*, English edition, no. 1981-3, 1981, pp. 21-45.
74. Stewartson, K.: Multistructured Boundary Layers on Flat Plates and Related Bodies, *Adv. in Appl. Mech.*, vol. 14, 1974.
75. Coles, D.: The Law of the Wake in the Turbulent Boundary Layer, *J. Fluid Mech.*, vol. 1, 1956, pp. 191-226.
76. Maise, G.; and McDonald, H.: Mixing Length and Kinematic Eddy Viscosity in a Compressible Boundary Layer, *AIAA J.*, vol. 6, 1968, pp. 73-80.
77. Adamson, T. C., Jr.; and Feo, A.: Interaction between a Shock Wave and a Turbulent Boundary Layer in Transonic Flow, *SIAM J. Appl. Math.*, vol. 29, 1975, pp. 121-145.
78. Inger, G. R.; and Mason, W. H.: Analytical Theory of Transonic Normal Shock-Boundary Layer Interaction, *AIAA J.*, vol. 14, 1976, pp. 1266-1272.
79. Stewartson, K.: Some Recent Studies in Triple-Deck Theory, First proceedings volume of *Numerical and Physical Aspects of Aerodynamic Flows*, T. Cebeci, ed., Springer-Verlag, 1982.

80. Oseen, C. W.: Ueber die Stokes'sche Formel, und über eine verwandte Aufgabe in der Hydrodynamik, *Ark. Math. Astronom. Fys.*, vol. 6, no. 29, 1910.
81. Van Dyke, M.: *Perturbation Methods in Fluid Mechanics*, Annotated ed., Parabolic Press, Stanford, Calif., 1975.
82. Kaplan, S.: The Role of Coordinate Systems in Boundary Layer Theory, *ZAMP*, vol. 5, 1954, pp. 111-135.
83. Davis, R. T.: A Study of Optimal Coordinates in the Solution of the Navier-Stokes Equations, Report AFL 74-12-14, Department of Aerospace Engineering., U. of Cincinnati, Cincinnati Ohio, 1974.
84. *An Album of Fluid Motion*, Assembled by M. Van Dyke, Parabolic Press, Stanford, Calif., 1982.
85. Brusseleers, M.: Physical and Numerical Aspects of Shock Boundary Layer Interactions, von Karman Institute for Fluid Dynamics Lecture Series 1980-8, *Shock-Boundary Layer Interaction in Turbomachines*, 1980.
86. Delery, J.: Some Features of Transonic Shock Wave Turbulent Boundary Layer Interaction, von Karman Institute for Fluid Dynamics Lecture Series 1980-8, *Shock-Boundary Layer Interaction in Turbomachines*, 1980.
87. Curle, N.: *The Laminar Boundary Layer Equations*, Oxford University Press, 1962.
88. Adamson, T. C.: The Structure of Shock Wave Boundary Layer Interactions in Transonic Flow, *IUTAM Symposium Transsonicum II*, K. Oswatitsch, and D. Rues, eds., Springer-Verlag, 1976.
89. Holder, D. W.: The Transonic Flow past Two-Dimensional Aerofoils, *J. R. Aeronaut. Soc.*, vol. 68, 1964, pp. 501-516.
90. Holder, D. W.; Pearcey, H. H.; and Gadd, G. W.: The Interaction between Shock Waves and Boundary Layers, Aeronautical Research Council, CP 180, Feb. 1954.
91. Ackeret, J.; Feldmann, F.; and Rott, N.: Investigations of Compression Shocks and Boundary Layers in Gases Moving at High Speeds, NACA TM-1113, 1947.
92. Bradshaw, P.: Complex Strain Fields, *The 1980-81 AFOSR-HTTM-Stanford Conference on Complex Turbulent Flows: Comparison of Computation and Experiment*, vol. 2, Taxonomies, Reporters' Summaries, Evaluation and Conclusions, S. J. Kline, B. J. Cantwell, and G. M. Lilley, eds., Thermoscience Division, Stanford U., Stanford, Calif., 1982.
93. Bradshaw, P.: Review - Complex Turbulent Flows, *Trans. ASME J. Fluid Eng.*, vol. 97, June 1975, pp. 146-154.
94. Emmons, H. W.: The Laminar-Turbulent Transition in a Boundary Layer, Part I, *J. Aeronaut. Sci.*, vol. 18, 1951, pp. 490-498.
95. Schubauer, G. B.; and KLEBANOFF, P. S.: Contributions on the Mechanics of Boundary Layer Transition, NACA TN-3489, 1955.

96. Coles, D. E.; and Barker, S. J.: Some Remarks on a Synthetic Turbulent Boundary Layer, *Turbulent Mixing in Nonreactive and Reactive Flows*, S. N. B. Murthy, ed., 1975, pp. 285-292.
97. Wygnanski I.; Sokolov, N.; and Freidman, D.: On the Turbulent "Spot" in a Boundary Layer Undergoing Transition, *J. Fluid Mech.*, vol. 78, 1976, pp. 785-819.
98. Wygnanski, I. J.; and Champagne, F. H.: On Transition in a Pipe, Part I, The Origin of Puffs and Slugs and the Flow in a Turbulent Slug, *J. Fluid Mech.*, vol. 59, 1973, pp. 281-335.
99. Corrsin, S.; and Kistler, A.: The Free Stream Boundaries of Turbulent Flows, NACA TN-3133, 1954. (Also NACA TR 1244, 1955.)
100. *Webster's New Collegiate Dictionary*, (s. v. coherent) G. & C. Merriam Company, 1976.
101. Favre, A. J.; Gaviglio, J. J.; and Dumas, R.: Space-Time Double Correlation and Spectra in a Turbulent Boundary Layer, *J. Fluid Mech.*, vol. 2, 1957, pp. 313-341.
102. Lumley, J. L.: Coherent Structures in Turbulence, *Transition and Turbulence*, R. E. Meyer, ed., Academic Press, 1981.
103. Hussain, A. K. M. F.: Coherent Structures - Reality and Myth, *Phys. Fluids*, vol. 26, no. 10, Oct. 1983, pp. 2816-2850.
104. Falco, R. E.: New Results, a Review and Synthesis of the Mechanism of Turbulence Production in Boundary Layers and its Modification, AIAA Paper 83-0377, Presented at 21st Aerospace Sciences Meeting, Reno, Nev., 1983.
105. Cantwell, B. J.: Organized Motion in Turbulent Flow, *Annu. Rev. Fluid Mech.*, vol. 13, 1981, pp. 457-515.
106. *Coherent Structure of Turbulent Boundary Layers*, C. R. Smith, and D. E. Abbott, eds., an AFOSR/Lehigh University Workshop, Nov. 1978.
107. Willmarth, W. W.; and Bogar, T. J.: Survey and New Measurements of Turbulent Structure Near the Wall, *Phys. Fluids*, vol. 20, no. 10, Pt. II, 1977, pp. S9-S21.
108. Willmarth, W. W.: Structure of Turbulence in Boundary Layers, *Adv. Appl. Mech.*, vol. 15, 1975, pp. 159-254.
109. Bakewell, H. P.; and Lumley, J. L.: Viscous Sublayer and Adjacent Region in Turbulent Pipe Flow, *Phys. Fluids*, vol. 10, 1967, pp. 1880-1889.
110. Blackwelder, R. F.: The Bursting Process in Turbulent Boundary Layers, *Coherent Structure of Turbulent Boundary Layers*, C. R. Smith, and D. E. Abbott, eds., an AFOSR/Lehigh University Workshop, Nov. 1978.
111. Praturi, A. K.; and Brodkey, R. E.: A Stereoscopic Visual Study of Coherent Structures in Turbulent Shear Flow, *J. Fluid Mech.*, vol. 89, 1978, pp. 251-272.

112. Blackwelder, R. F.; and Eckelmann, H.: Streamwise Vortices Associated with the Bursting Phenomenon, *J. Fluid Mech.*, vol. 94, 1979, pp. 577-594.
113. Gupta, A. K.; Laufer, J.; and Kaplan, R. E.: Spatial Structure in the Viscous Sublayer, *J. Fluid Mech.*, vol. 50, 1971, pp. 493-512.
114. Kline, S. J., Reynolds, W. C., Schraub, F. A., and Runstadler, P. W.: The Structure of Turbulent Boundary Layers, *J. Fluid Mech.*, vol. 30, 1967, pp. 741-773.
115. Rao, K. N.; Narasimha, R.; and Narayanan, M. A. B.: Bursting in a Turbulent Boundary Layer, *J. Fluid Mech.*, vol. 48, 1971, pp. 339-352.
116. Blackwelder, R. F.; and Haritonidis, J. H.: Scaling of the Bursting Frequency in Turbulent Boundary Layers, *J. Fluid Mech.*, vol. 132, 1983, pp. 87-103.
117. Willmarth, W. W.; and Lu, S. S.: Structure of the Reynolds Stress Near the Wall, *J. Fluid Mech.*, vol. 55, 1972, pp. 65-69.
118. Falco, R. E.: Coherent Motions in the Outer Region of Turbulent Boundary Layers, *Phys. Fluids*, vol. 20, no. 10, 1977, pp. S124-S132.
119. Hinze, J. O.: *Turbulence*, Second ed., McGraw-Hill, Inc., 1975.
120. Preston, J. H.: The Minimum Reynolds Number for a Turbulent Boundary Layer and the Selection of a Transition Device, *J. Fluid Mech.*, vol. 3, 1958, p. 373.
121. *The 1980-81 AFOSR-HTTM-Stanford Conference on Complex Turbulent Flows : Comparison of Computation and Experiment*, vol. 2, Taxonomies, Reporters' Summaries, Evaluation and Conclusions, S. J. Kline, B. J. Cantwell, and G. M. Lilley, eds., Thermoscience Division, Stanford U., Stanford, Calif., 1982.
122. Coles, D. E.: The Turbulent Boundary Layer in a Compressible Fluid, R-403-PR, Rand Corp., Los Angeles, Calif., 1962. (Also, AD 285-651.)
123. Murlis, J.; Tsai, H. M.; and Bradshaw, P.: The Structure of Turbulent Boundary Layers at Low Reynolds Numbers, *J. Fluid Mech.*, vol. 122, 1962, pp.13-56.
124. Cebeci, T.; and Bradshaw, P.: *Momentum Transfer in Boundary Layers*, Hemisphere Publishing Corporation, Washington, D. C., 1977.
125. Burggraf, O. R., Rizzetta, D., Werle, M. J., and VASTA, V. N.: Effect of Reynolds Number on Laminar Separation of a Supersonic Stream, *AIAA J.*, vol. 17, 1979, pp. 336-343.
126. Inger, G. R.: Nonasymptotic Theory of Unseparated Turbulent Boundary Layer-Shock Wave Interactions with Application to Transonic Flows, First proceedings volume of *Numerical and Physical Aspects of Aerodynamic Flows*, T. Cebeci, ed., Springer-Verlag, 1982.
127. Inger, G. R.: Some Features of a Shock-Turbulent Boundary Layer Interaction Theory in Transonic Flow Fields, Paper no. 18, AGARD CP-291, 1980.

128. Granville, P. S.: The Determination of the Local Skin Friction and the Thickness of Turbulent Boundary Layers from the Velocity Similarity Laws, R & D Report 1340, Dept. of the Navy, David Taylor Model Basin, Hydromechanics Laboratory, Bethesda, Maryland, Oct. 1959.
129. Taylor, G. I.; and Maccoll, J. W.: The Mechanics of Compressible Fluids, in *Aerodynamic Theory -- A General Review of Progress*, Vol. 3, W. F. Durand, ed., Dover Publications, Inc., New York, 1963.
130. Lagerstrom, P. A.: Laminar Flow Theory, *Theory of Laminar Flows*, Vol. IV. High Speed Aerodynamics and Jet Propulsion, F. K. Moore, ed., Princeton University Press, Princeton, N. J., 1964.
131. Sherman, F. S.: A Low-Density Wind-Tunnel Study of Shock-Wave Structure and Relaxation Phenomena in Gases, NACA TN-3298, 1955.
132. Monin, A. S.; and Yaglom, A. M., *Statistical Fluid Mechanics of Turbulence*, Vol. 1, MIT Press, Cambridge, Mass., 1971, pp. 205-209.
133. Acharya, M.; and Reynolds, W. C.: Measurements and Prediction of a Fully Developed Turbulent Channel Flow with Imposed Controlled Oscillations, Report TF-8, Mechanical Engineering Department, Stanford U., Stanford, Calif., 1975.
134. Karlsson, S. K. F.: An Unsteady Turbulent Boundary Layer, Ph. D. thesis, Johns Hopkins U., Baltimore, Md., 1958.
135. Ramaprian, B. R.; and Tu, S.-W.: An Experimental Study of Oscillatory Pipe Flow at Transitional Reynolds Numbers, *J. Fluid Mech.*, vol. 100, 1980, pp. 513-544.
136. Mizushima, T., Maruyama, T., and Shiozaki, Y.: Pulsating Turbulent Flow in a Tube, *Journal of Chemical Engineering of Japan*, vol. 6, no. 6, 1973.
137. Cousteix, J.; Houdeville, R.; and Raynaud, M.: Oscillating Turbulent Boundary Layer with Strong Mean Pressure Gradient, *Turbulent Shear Flows*, Vol. 2, F. Durst, B. E. Launder, F. W. Schmidt, L. J. S. Bradbury, and J. H. Whitelaw, Springer-Verlag, 1980.
138. Parikh, P. G.; Reynolds, W. C.; and Jayaraman, R.: On the Behavior of an Unsteady Turbulent Boundary Layer, First proceedings volume *Numerical and Physical Aspects of Aerodynamic Flows*, T. Cebeci, ed., 1982.
139. Simpson, R. L.; Chew, Y. T.; and Shivaprasad, B. G.: Measurements of Unsteady Turbulent Boundary Layers with Pressure Gradients, SMU Report WT-6, Southern Methodist U., Dallas, Tex., Aug. 1980.
140. Cousteix, J.; and Houdeville, R.: Effects of Unsteadiness on Turbulent Boundary Layers, von Karman Institute for Fluid Dynamics, Lecture Series 1983-03, Turbulent Shear Flows, 1983.
141. Carr, L. W.: A Review of Unsteady Turbulent Boundary-Layer Experiments, NASA TM-81297, 1981.

142. Chapman, D. R.: Computational Aerodynamics Development and Outlook, *AIAA J.*, vol. 17, 1979, pp. 1293-1313.
143. Lugt, H. J.: The Vortex Concept in the History of Science, CMD-04-76, David W. Taylor, Naval Ship Research and Development Center, Bethesda, Maryland, Jan. 1976.
144. Serrin, J.: Mathematical Principles of Classical Fluid Mechanics, *Handbuch der Physik*, Band VIII/1, Springer-Verlag, 1959.
145. Truesdell, C. A.: *Kinematics of Vorticity*, Indiana University Press, Bloomington, Ind., 1954.
146. Saffman, P. G.; and Baker, G. R.: Vortex Interactions, *Annu. Rev. Fluid Mech.*, vol. 11, 1979, pp. 95-122.
147. Mehta, U.; and Lavan, Z.: Starting Vortex, Separation Bubbles and Stall: A Numerical Study of Laminar Unsteady Flow around an Airfoil, *J. Fluid Mech.*, vol. 67, 1975, pp. 227-256.
148. Mehta, U.: Dynamic Stall of an Oscillating Airfoil, *Unsteady Aerodynamics*, Paper No. 23, AGARD CP-227, September 1977.
149. Lugt, H. J.: *Vortex Flow in Nature and Technology*, John Wiley & Sons, Inc., New York, 1983.
150. Lugt, H. J.: The Dilemma of Defining a Vortex, *Recent Developments in Theoretical and Experimental Fluid Mechanics*, Springer-Verlag, New York, 1979, p. 309.
151. Küchmann, D.: Report on the IUTAM Symposium on Concentrated Vortex Motions in Fluids, *J. Fluid Mech.*, vol. 21, 1965, pp. 1-20.
152. Peake, D. J.; and Tobak, M.: Three-Dimensional Interactions and Vortical Flows with Emphasis on High Speeds, AGARD-AG-252, July 1980.
153. Roshko, A.: The Plane Mixing Layer: Flow Visualization Results and Three-Dimensional Effects, Proceedings of an International Conference on the Role of Coherent Structures in Modelling Turbulence and Mixing, Madrid, Spain, June 1981.
154. Kelvin, Lord (Thomson, W.): On Vortex Motion, *Mathematics and Physics Papers*, vol. 4, 1869, p. 49.
155. Lighthill, M. J.: Introduction. Boundary Layer Theory, *Laminar Boundary Layers*, L. Rosenhead, ed., Oxford University Press, 1963.
156. Batchelor, G. K.: *An Introduction to Fluid Dynamics*, Cambridge University Press, 1967.
157. Vazsonyi, A.: On Rotational Gas Flows, *Q. J. Appl. Math.* vol. 3, no. 1, Apr. 1945, pp. 29-37.

158. Hadamard, J.: Sur les Tourbillons Produit par les Ondes de Choc, Note III, *Lecons sur la Propagation des Ondes*, A. Hermann, ed., Paris, 1903, p. 362.
159. Tennekes, H.; and Lumley, J. L.: *A First Course in Turbulence*, MIT Press, Cambridge, Mass., 1972.

| | | | |
|---|--|---|-----------------------|
| 1. Report No. NASA TM 85893 | 2. Government Accession No. | 3. Recipient's Catalog No. | |
| 4. Title and Subtitle PHYSICAL ASPECTS OF COMPUTING THE FLOW OF A VISCOUS FLUID | | 5. Report Date | |
| | | 6. Performing Organization Code | |
| 7. Author(s) Unmeel B. Mehta | | 8. Performing Organization Report No. A-9650 | |
| | | 10. Work Unit No. T-6465 | |
| 9. Performing Organization Name and Address Ames Research Center Moffett Field, Calif. 94035 | | 11. Contract or Grant No. | |
| | | 13. Type of Report and Period Covered Technical Memorandum | |
| 12. Sponsoring Agency Name and Address National Aeronautics and Space Administration Washington, DC 20546 | | 14. Sponsoring Agency Code 505-31-01 | |
| | | | |
| 15. Supplementary Notes Point of contact: Unmeel B. Mehta, Ames Research Center, MS 202A-1, Moffett Field, CA 94035 (415) 965-5548 or FTS 448-5548 | | | |
| 16. Abstract One of the main themes in fluid dynamics at present and in the future is going to be computational fluid dynamics with the primary focus on the determination of drag, flow separation, vortex flows, and unsteady flows. A computation of the flow of a viscous fluid requires an understanding and consideration of the physical aspects of the flow. This is done by identifying the flow regimes and the scales of fluid motion, and the sources of vorticity. Discussions of flow regimes deal with conditions of incompressibility, transitional and turbulent flows, Navier-Stokes and non-Navier-Stokes regimes, shock waves, and strain fields. Discussions of the scales of fluid motion consider transitional and turbulent flows, thin- and slender-shear layers, triple- and four-deck regions, viscous-inviscid interactions, shock waves, strain rates, and temporal scales. In addition, the significance and generation of vorticity are discussed. These physical aspects mainly guide computations of the flow of a viscous fluid. | | | |
| 17. Key Words (Suggested by Author(s)) Viscous flows, Boundary layers, Viscous/ inviscid interactions, Transition, Turbulent flows, Shock waves, Vortex flows, Separated flows, Unsteady flows | | 18. Distribution Statement Unlimited Subject Category: 02 | |
| 19. Security Classif. (of this report) Unclassified | 20. Security Classif. (of this page) Unclassified | 21. No. of Pages 50 | 22. Price* A03 |